Undulator Tapering

M.V. Yurkov
DESY, Hamburg

I. Introduction.
II. Undulator with linear taper.
III. Reverse undulator tapering.
IV. Undulator tapering for efficiency increase in the presence of diffraction effects.

Tapering

Wikipedia:

… In mathematics, physics, and theoretical computer graphics, tapering is a kind of shape deformation.

… Acoustic resonance is an important consideration for instrument builders, as most acoustic instruments use resonators, such as the strings and body of a violin, the length of tube in a flute, and the shape of a drum membrane. Acoustic resonance is also important for hearing. For example, resonance of a stiff structural element, called the basilar membrane within the cochlea of the inner ear allows hair cells on the membrane to detect sound. (For mammals the membrane has tapering resonances across its length so that high frequencies are concentrated on one end and low frequencies on the other.)

FEL physics:

In the context of free electron lasers, undulator tapering refers to variation of undulator parameters along the undulator (field and (or) period) in order to control resonance properties of the amplification process.

Practical use of undulator tapering

- Positive tapering: undulator K decreases along the undulator length. Can be used for:
  - Compensation of the beam energy loss due to spontaneous undulator radiation;
  - Compensation of the energy chirp in the electron beam;
  - Increase power of a high-gain FEL after saturation (post-saturation taper).
- Negative (reverse) tapering: undulator K increases along the undulator length. Can be used for:
  - Compensation of the energy chirp in the electron beam;
  - Suppression of the radiation from the main undulator for organization of effective operation of afterburners (e.g., circular polarization).
  - Application in the scheme of attosecond SASE FEL.
  - Increase power of FEL oscillator.

A concept of post-saturation undulator tapering

- Resonance condition: Electromagnetci wave advances the electron by one wavelength when electron passes one undulator period:

$$\frac{\lambda_w}{v_z} = \frac{\lambda}{c - v_z}, \qquad \lambda \simeq \frac{\lambda_w}{2\gamma_z^2} = \lambda_w \frac{1 + K^2}{2\gamma^2}.$$

- Undulator tapering: originally proposed by [N.M. Kroll, P.L. Morton, and M.N. Rosenbluth, IEEE J. Quantum Electronics, QE-17, 1436 (1981)] for increasing the radiation power in the post-saturation regime preserving resonance condition:

$$\lambda \simeq \lambda_w(z) \frac{1 + K^2(z)}{2\gamma^2(z)}.$$

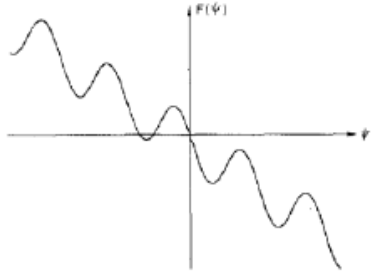

Fig. 1. The poderomotive potential $F(\psi)$. The case shown is for positive ψ_r corresponding to the case in which energy is extracted from the electrons.

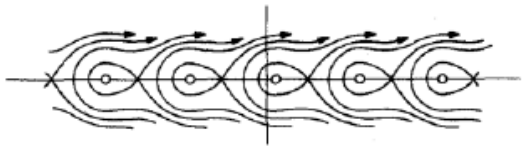

Fig. 2. Trajectories in the ψ, $\delta\gamma$ phase plane for $\psi_r > 0$.

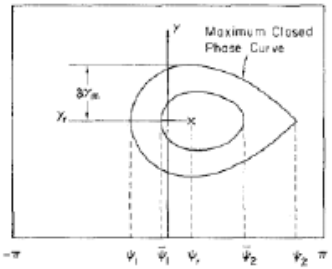

Fig. 3. Stable phase plane trajectories.

change in parameters is small. For small oscillations about ψ_r, one can expand $F(\psi)$ about ψ_r. The motion for these orbits is harmonic with period of oscillation

$$Z = \frac{\pi\mu}{(k_w + \delta k_s)\sqrt{a_s a_w \cos\psi_r}} \approx \frac{\mu\lambda_w}{2\sqrt{a_s a_w \cos\psi_r}}$$

$(\lambda_w \equiv 2\pi/k_w).$ (2.50)

Experimental verification of the undulator tapering at LLNL: FEL amplifier

Successful experiment at LLNL with seeded FEL amplifier (1 cm wavelength).
T.J. Orzechowski et al. Phys. Rev. Lett. 57, 2172-2175 (1986)

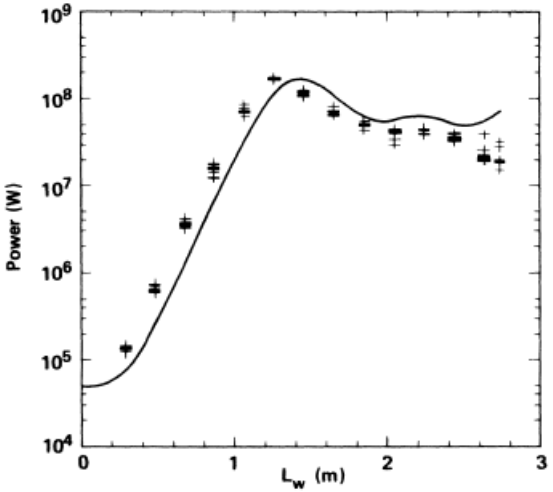

FIG. 1. Amplified signal output as a function of wiggler length for uniform (flat) wiggler. Crosses indicate experimental values and the solid line is the result of numerical evaluation.

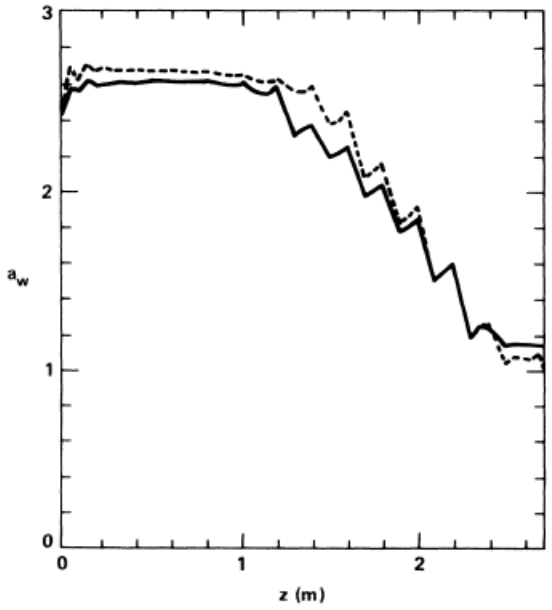

FIG. 2. Optimum wiggler field profile for tapered wiggler. The dashed line corresponds to empirical evaluation and the solid line is the numerical prediction.

doing the computer design, the wiggler was con-

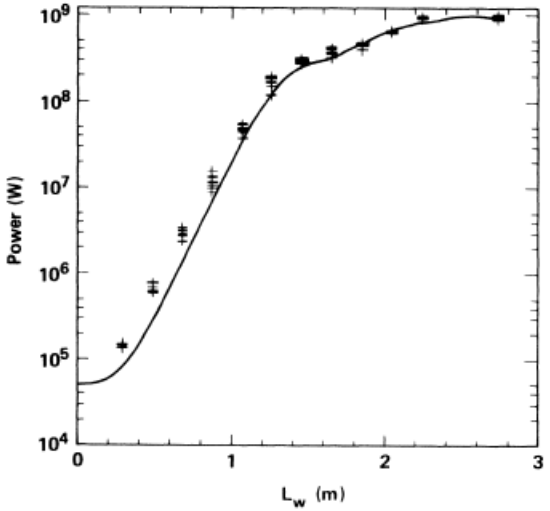

FIG. 3. Amplified signal output as a function of wiggler length for tapered wiggler field. Crosses indicate experimental values and the solid line is the results of the numerical evaluation.

Experimental verification of the undulator tapering at Jefferson Lab: FEL oscillator

First experiments with FEL oscillators indicated that tapering proposed by Kroll, Morton and Rosenbluth does not work well as for FEL amplifier. Our analysis (E.L. Saldin, E.A. Schneidmiller, M.V. Yurkov, Opt. Commun. 103, 297 (1993); NIM A 375, 336 (1996)) have shown that in the case of FEL oscillator the lasing frequency is defined by the condition of the maximum amplification in the small-signal regime. The position of the amplification maximum depends on the depth of the tapering. At some values of the depth of the tapering this effect leads to the significant decrease of the FEL oscillator efficiency when the undulator parameters are tapered in the same way as in the FEL amplifier. In some cases quite a different way of tapering is more preferable, for instance, with the undulator field increase at the fixed period (so called negative tapering). Dedicated experiments at Jefferson IR FEL confirmed this feature.

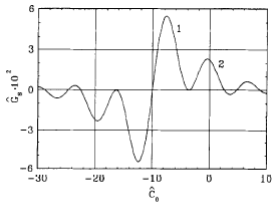

Fig. 1. The reduced small-signal gain versus the reduced detuning at the undulator entrance. Here $\hat{b} = 20$. (1) – the first maximum, (2) – the second maximum.

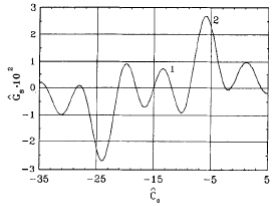

Fig. 2. The reduced small-signal gain versus the reduced detuning at the undulator entrance. Here $\hat{b} = 30$. (1) – the first maximum, (2) – the second maximum.

ELSEVIER Nuclear Instruments and Methods in Physics Research A 475 (2001) 276–280

SECTION A

www.elsevier.com/locate/nima

An experimental study of an FEL oscillator with a linear taper

S. Benson*, J. Gubeli, G.R. Neil

Jefferson Lab, MS 6A, 12000 Jefferson Ave., TJNAF, Newport News, VA 23606, USA

Abstract

Motivated by the work of Saldin, Schneidmiller and Yurkov, we have measured the detuning curve widths, spectral characteristics, efficiency, and energy spread as a function of the taper for low and high Q resonators in the IR Demo FEL at Jefferson Lab. Both positive and negative tapers were used. Gain and frequency agreed surprisingly well with the predictions of a single mode theory. The efficiency agreed reasonably well for a negative taper with a high Q resonator but disagreed for lower Q values both due to the large slippage parameter and the non-ideal resonator Q. We saw better efficiency for a negative taper than for the same positive taper. The energy spread induced in the beam, normalized to the efficiency is larger for the positive taper than for the corresponding negative taper. This indicates that a negative taper is preferred over a positive taper in an energy recovery FEL.

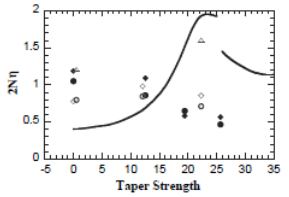

Fig. 2. The experimental normalized efficiency $2N\eta$ vs. taper strength is shown. The curve is scaled from the one in Ref. [8]. The circles are CW efficiencies, the diamonds are pulsed efficiency and the triangles are the pulsed efficiency for the case of $Q = 50$. The filled symbols are taken at 3 μm and the empty ones at 6 μm. Two of the symbols are slightly offset at $b = 0$ for clarity.

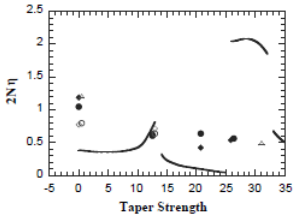

Fig. 3. The experimental normalized efficiency vs. taper strength for a positive taper is shown. The curve is scaled from Ref. [8]. The symbol definition is the same as for Fig. 2.

Outline

I. Introduction.

II. Undulator with linear taper.

III. Reverse undulator tapering.

IV. Undulator tapering for efficiency increase in presence of diffraction effects.

Linear undulator tapering

Parameters of 1D FEL theory:

$$\widehat{C} = \frac{1}{\Gamma}\left[\frac{2\pi}{\lambda_w} - \frac{2\pi}{\lambda}\frac{1+K^2}{2\gamma^2}\right] \quad - \quad \text{The detuning parameter.}$$

$$\hat{z} = \Gamma z \quad - \quad \text{Normalized coordinate } z.$$

$$\Gamma = \frac{4\pi\rho}{\lambda_w} \quad - \quad \text{The gain parameter.}$$

Linear undulator tapering:

$$\widehat{C}(\hat{z}) = \hat{\beta}\hat{z} \qquad \hat{\beta} = -\frac{\lambda_w}{4\pi\rho^2}\frac{K(0)}{1+K(0)^2}\frac{dK}{d\hat{z}}$$

Equivalence of the undulator tapering and the energy chirp

- There is a symmetry between the energy chirp and the undulator tapering (E.L. Saldin, E.A. Schneidmiller, M.V. Yurkov, Phys. Rev. ST Accel. Beams 9, 050702 (2006)):

$$\hat{\alpha} = -\frac{d\gamma}{dt}\frac{1}{\gamma_0\omega_0\rho^2}\,, \qquad \hat{C}(\hat{z}) = \hat{\beta}\hat{z}$$

- If we look at the radiation field acting on some test electron from an electron behind it, this field was emitted at a retarded time. In first case a radiating electron has a detuning due to an energy offset, in the second case it has the same detuning because undulator parameters were different at a retarded time.

- Question: Can these two effects compensate each other?
- Answer: Yes, if:

$$\frac{1}{H_{w0}}\frac{dH_w}{dz} = -\frac{1}{2}\frac{(1+K_0^2)^2}{K_0^2}\frac{1}{\gamma_0^3}\frac{d\gamma}{cdt}$$

Red line: $\hat{\alpha}=0$, $\hat{\beta}=0$; triangles: $\hat{\alpha}=4$, $\hat{\beta}=-2$
Blue line: $\hat{\alpha}=4$, $\hat{\beta}=0$; circles: $\hat{\alpha}=0$, $\hat{\beta}=2$

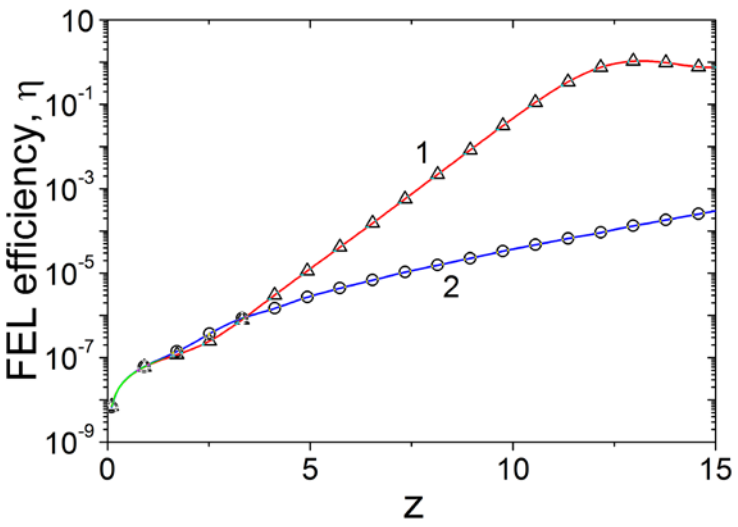

SASE FEL: frequency shift

- In a SASE FEL the evolution of the amplified frequency band depends on tapering.
- For weak tapering, $|\hat{\beta}| \ll 1$, the central frequency follows change of resonance frequency (due to K or energy change) with half of the rate (Z.Huang and G. Stupakov, Phys. Rev. ST-AB 040702(2005)8).
- For strong tapering, there is no symmetry. For positive parameter, the frequency follows the change of resonance completely. For negative parameter, it doesnt follow current resonance at all; it stays at the resonance with undulator parameters at its entrance.

$\hat{\beta} < 0$

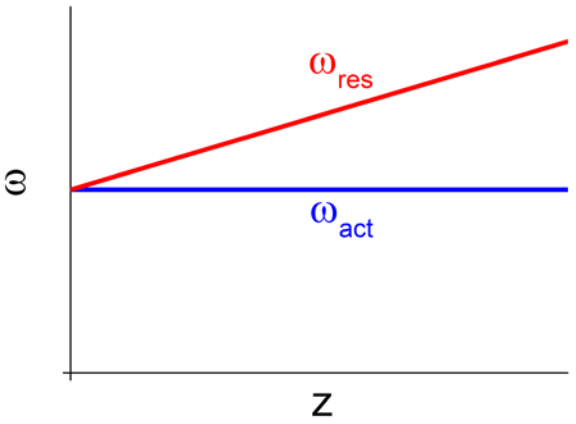

$\hat{\beta} > 0$

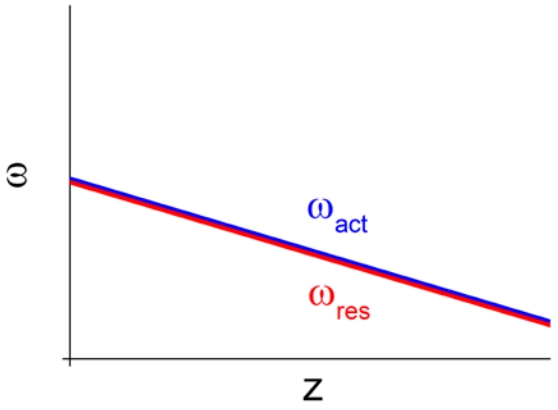

Linear tapering: Gain and saturation power of SASE FEL

- Detuning paremeter:

$$\hat{C} = [2\pi/\lambda_w - \omega/(2c\gamma_z^2)]/\Gamma \ , \qquad \Gamma = 4\pi\rho/\lambda_w$$

- SASE FEL with linear undulator tapering,

$$\hat{C}(\hat{z}) = \beta\hat{z} \ , \qquad \beta = -\frac{\lambda_w}{4\pi\rho^2}\,\frac{K(0)}{1+K(0)^2}\,\frac{dK}{dz} \ , \qquad \hat{z} = \Gamma z \ ,$$

- Saturation power of a SASE FEL with negative undulator tapering is significantly suppressed (E.L. Saldin, E.A. Schneidmiller, M.V. Yurkov, Phys. Rev. ST Accel. Beams 9, 050702 (2006)).
- Bunching is at a high level (E.A. Schneidmiller, M.V. Yurkov, Phys. Rev. ST Accel. Beams 16, 110702 (2013)).

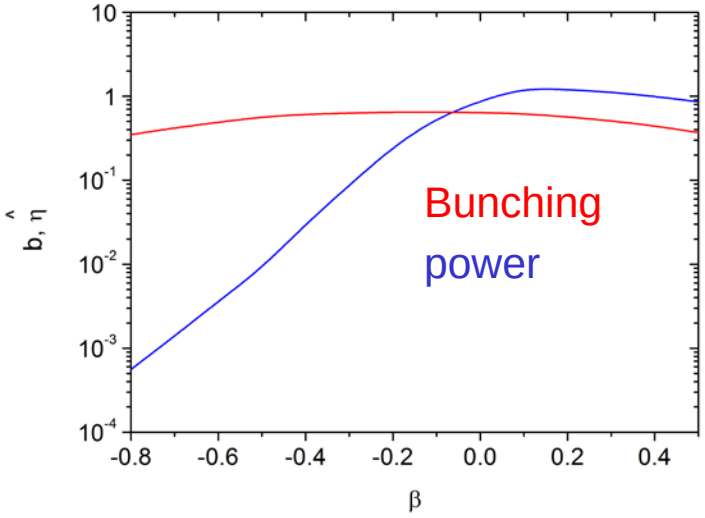

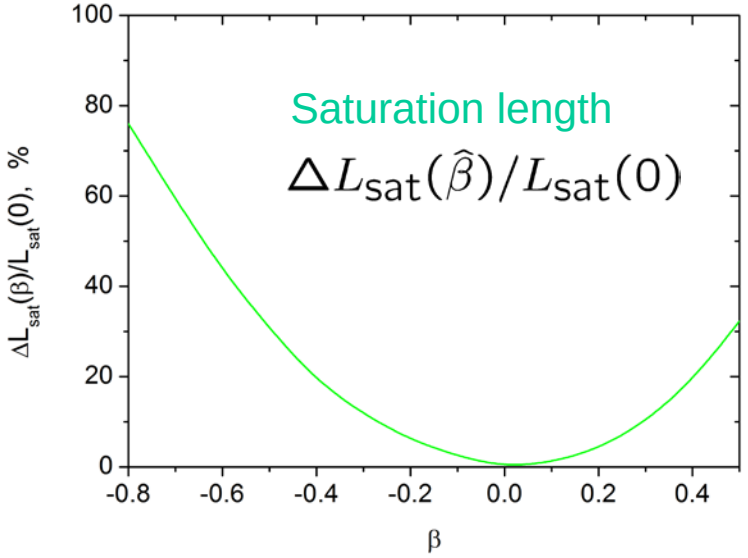

Outline

I. Introduction.

II. Undulator with linear taper.

III. Reverse undulator tapering.

IV. Undulator tapering for efficiency increase in presence of diffraction effects.

European XFEL

Location	Full length	Undulator
XS1-XS3	620 m	SASE1
XS3-XHDU1	301 m	SASE3
XS1-XS2	550 m	SASE2
XS2-XS4	190 m	Spont. U1
XS4-XHDU2	250 m	Spont. U2

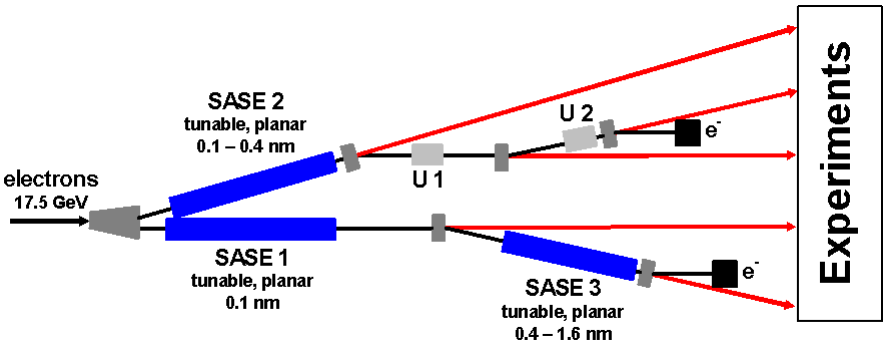

Photo by Dirk Noelle

Baseline option:

- 3 FEL beamlines (SASE1/2/3) cover 0.05 nm – 5 nm wavelength range
- Burst mode of operation: 10 x 0.6 ms pulse trains per second, 2700 pulses per train
- Laser lab is foreseen for pump-probe experiments (FEL+Laser)
- Need in sub-femtosecond pulses.
- Only linear polarization, but variable polarization is strongly requested by users.

Application of reverse tapering in a scheme for production of attosecond pulses

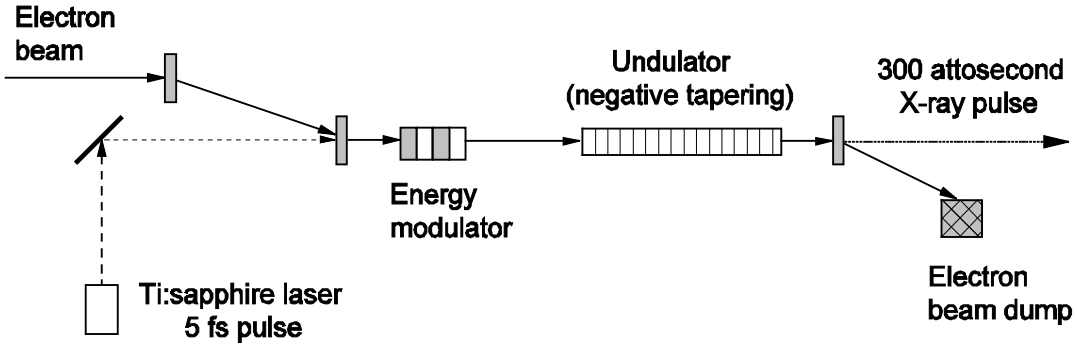

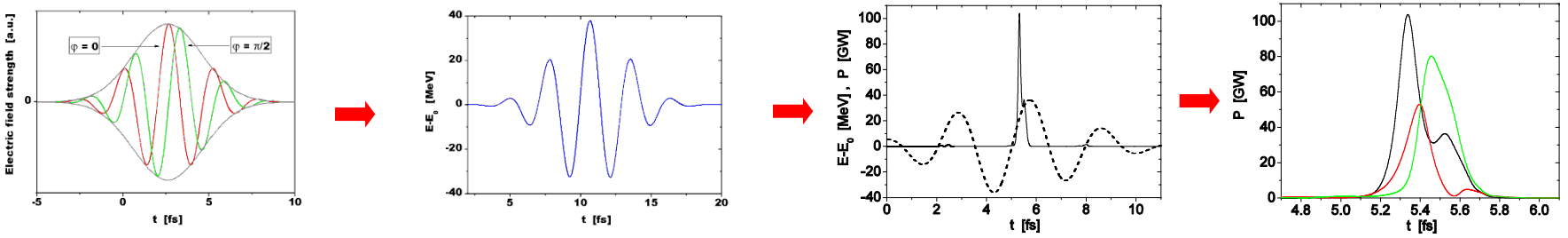

Slicing of electron bunch with fs-laser

SASE process

Strong energy modulation within a short slice of an electron bunch is produced by few-cycle optical laser pulse in a short undulator, placed in front of the main undulator. Gain degradation within this slice is compensated by an appropriate undulator taper while the rest of the bunch suffers from this taper and does not lase. Three-dimensional simulations predict that short (200 attoseconds) high-power (up to 100 GW) pulses can be produced in Angstroem wavelength range with a high degree of contrast.

E.L. Saldin, E.A. Schneidmiller, M.V. Yurkov, Phys. Rev. ST AB 9(2006)050702

Application of reverse tapering for effective operation of a helical afterburner

SASE3:

Electron beam	
Energy	14 GeV
Charge	0.5 nC
Peak current	5 kA
Rms normalized slice emittance	0.7 μm
Rms slice energy spread	2.2 MeV
Planar undulator	
Period	6.8 cm
K_{rms}	5.7
Beta-function	15 m
Active magnetic length	55 m
Taper $\Delta K_{\mathrm{rms}}/K_{\mathrm{rms}}(0)$	2.1 %
Helical afterburner	
Period	16 cm
K	3.6
Beta-function	15 m
Magnetic length	10 m
Radiation	
Wavelength	1.5 nm
Power from planar undulator, P_{lin}	0.4 GW
Power from helical undulator, P_{cir}	155 GW
$1 - P_{\mathrm{lin}}/(2P_{\mathrm{cir}})$	99.9 %

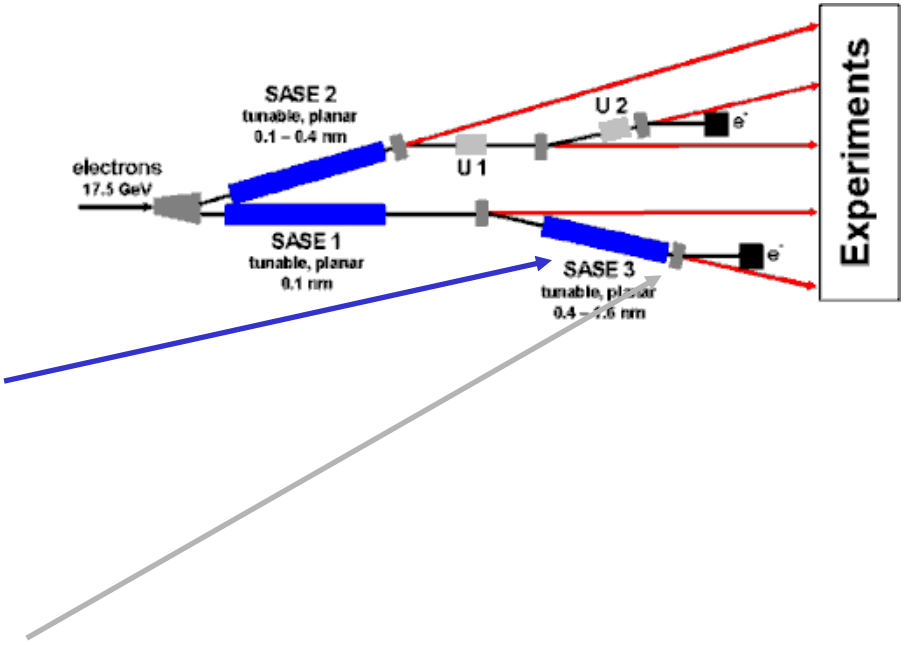

E.A. Schneidmiller and M.V. Yurkov, Phys. Rev. ST-AB 110702(2013)16

Application of reverse tapering for effective operation of a helical afterburner

reverse-tapered planar undulator (saturation) | helical AB

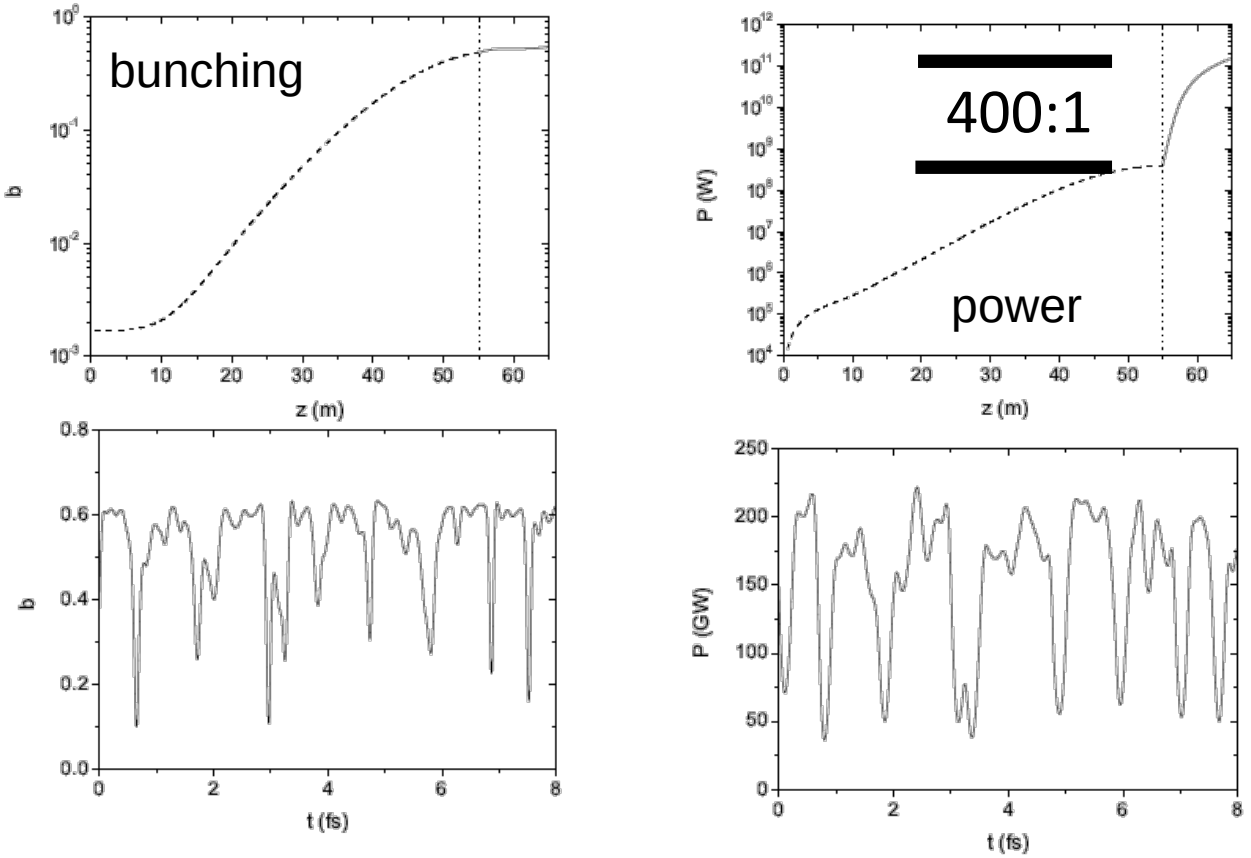

- Fully microbunched electron beam but strongly suppressed radiation power at the exit of reverse-tapered planar undulator
- The beam radiates at full power in the helical afterburner tuned to the resonance.

E.A. Schneidmiller and M.V. Yurkov, Phys. Rev. ST-AB 110702(2013)16

Application of reverse tapering for effective operation of a helical afterburner: 3D bonus

- It turned out that suppression by the reverse tapering of the radiation power in 3D case is more effective that in 1D case.
- The reason for this is that transverse mode gets more narrow for negative detuning. Thus, the field acting on particles is stronger for the same power.

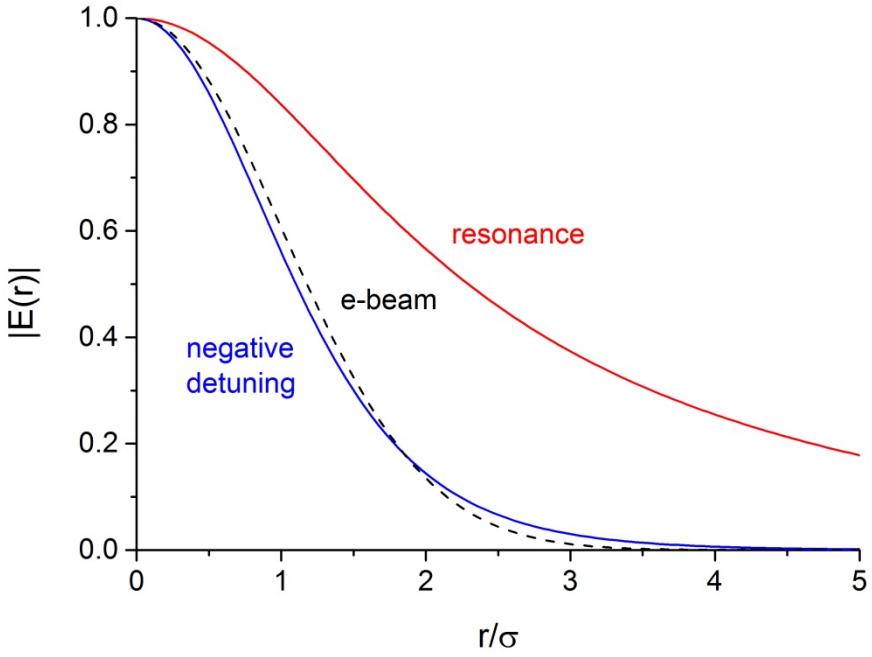

B = 0.1

C = 0

C=-20

E.A. Schneidmiller and M.V. Yurkov, Phys. Rev. ST-AB 110702(2013)16

Reverse taper at LCLS (2014)

- Helical afterburner (DELTA) will be installed at LCLS this fall for production of circularly polarized radiation
- First tests with reverse tapered undulator and planar afterburner were performed recently
- In the best case the power ratio 15:1 was obtained; this would correspond to the ratio 30:1 with helical afterburner

Poster TUP035 by J. MacArthur et al.

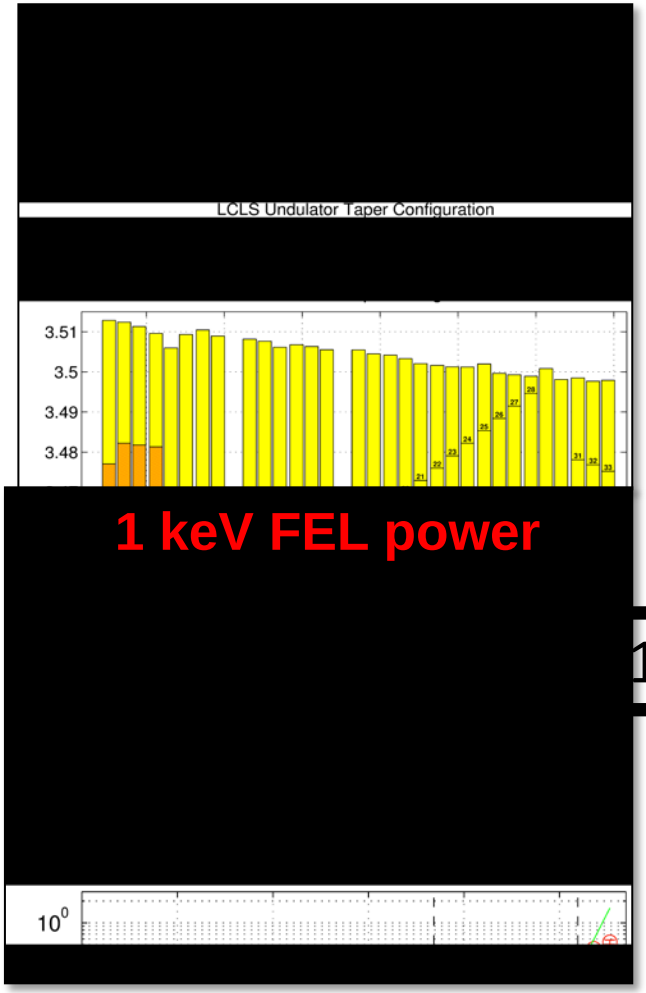

Courtesy Z. Huang

Reverse taper at LCLS (2015)

FEL2015 Daejeon Korea, 23rd – 28th August 2015

Heinz-Dieter Nuhn

Reverse Taper

E.A. Schneidmiller, M.V. Yurkov, “Obtaining high degree of circular polarization at X-ray FELs via a reverse undulator taper”, arXiv:1308.3342

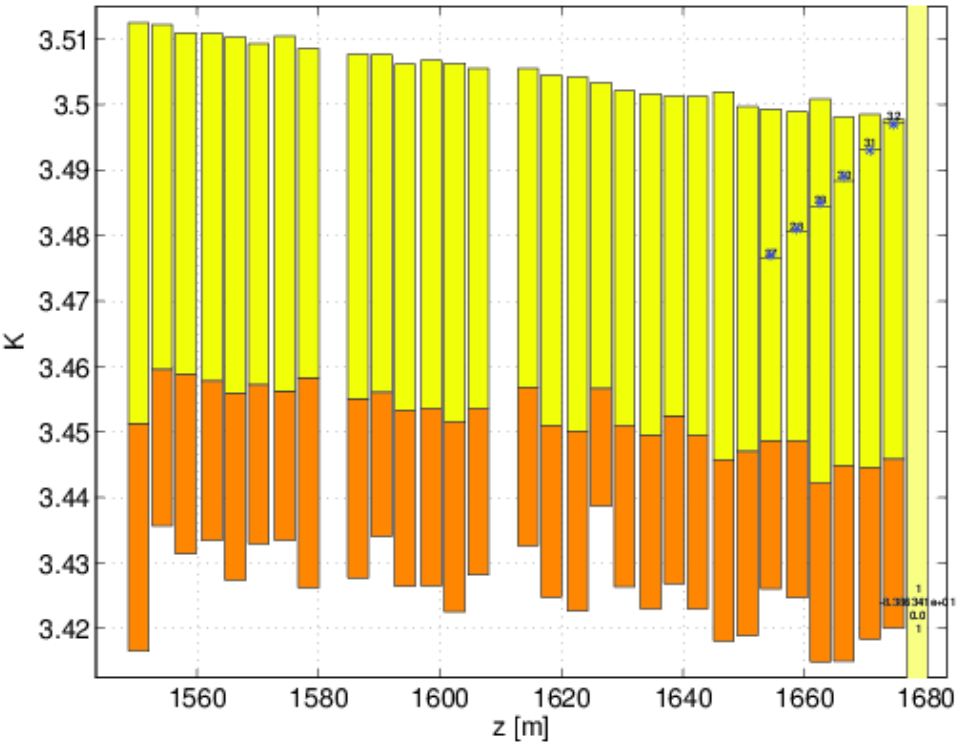

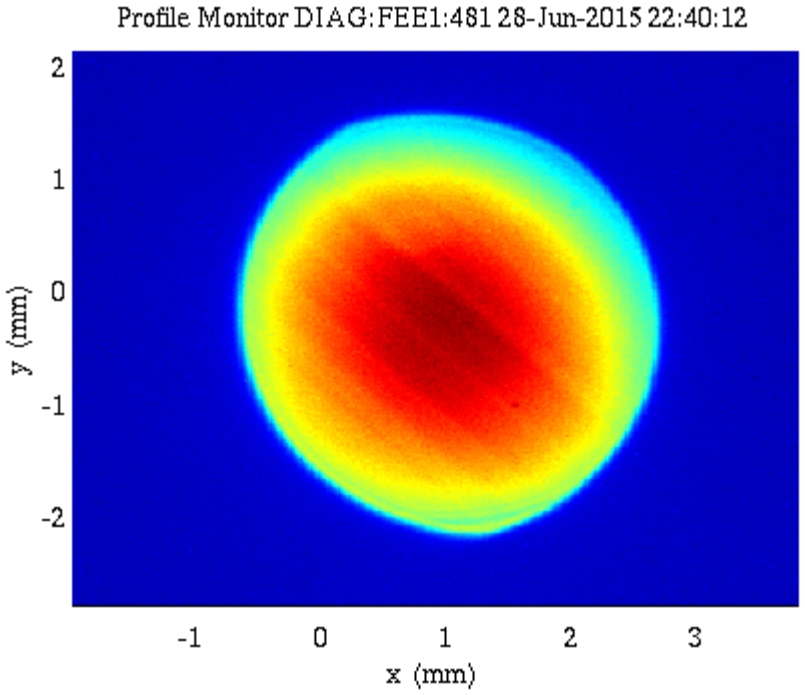

- X-ray growth suppressed during reverse taper

- 30 µJ with Delta off
- 510 µJ with Delta on

Peak Current increased above 4 kA

Courtesy H.D. Nuhn

James MacArthur WEP004

Advanced developments
Reverse undulator tapering

Experiment at FLASH2 on 23.01.2016

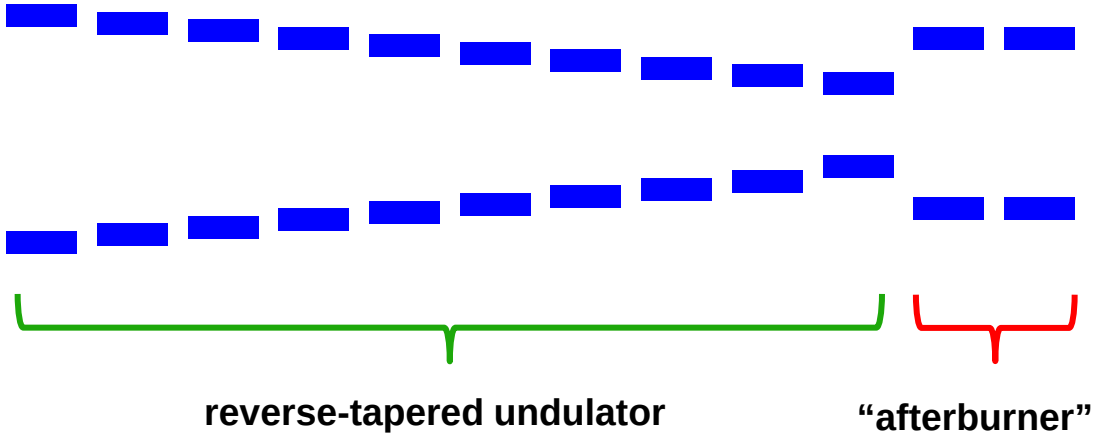

- Beam energy 720 MeV,
- Wavelength 17 nm.
- Reverse taper of 10% along 10 undulator segments;
- The gap of the 11th and 12th segments was scanned.
- Power ratio of 200 was obtained. For a helical afterburner it would be larger by a factor of 2.

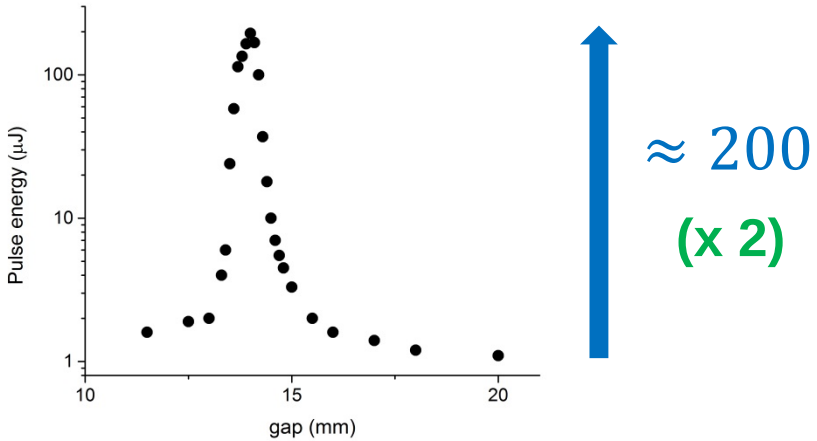

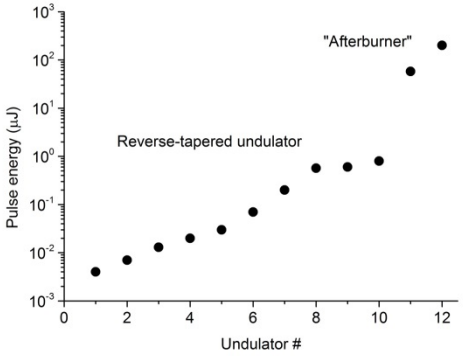

E. Schneidmiller and M. Yurkov, Proc. IPAC2016, MOPOW008

Undulator tapering in the presence of diffraction effects

- The problem of optimum undulator tapering in the presence of diffraction effects is now a “hot” topic due to practical applications for X-ray FELs and potential industrial applications.

- Empirical tapering dependencies for known so far from the literature are physically inconsistent with the asymptotical behavior of the radiation power produced in the tapered section.

- Here we present our view of the problem based on the recent findings:

– *Optimization of a high efficiency free electron laser amplifier, Phys. Rev. ST AB, 18, 030705 (2015);*
– *The universal method for optimization of undulator tapering in FEL amplifiers, Proc. of SPIE Vol. 9512 951219-1 (2015);*
– *Statistical properties of the radiation from SASE FEL operating in a post-saturation regime with and without undulator tapering, J. Modern Optics, DOI:10.1080/09500340.2015.1035349 (2015).*

A concept of post-saturation undulator tapering

- Resonance condition: Electromagnetci wave advances the electron by one wavelength when electron passes one undulator period:

$$\frac{\lambda_w}{v_z} = \frac{\lambda}{c - v_z}, \qquad \lambda \simeq \frac{\lambda_w}{2\gamma_z^2} = \lambda_w \frac{1 + K^2}{2\gamma^2}.$$

- Undulator tapering: originally proposed by [N.M. Kroll, P.L. Morton, and M.N. Rosenbluth, IEEE J. Quantum Electronics, QE-17, 1436 (1981)] for increasing the radiation power in the post-saturation regime preserving resonance condition:

$$\lambda \simeq \lambda_w(z) \frac{1 + K^2(z)}{2\gamma^2(z)}.$$

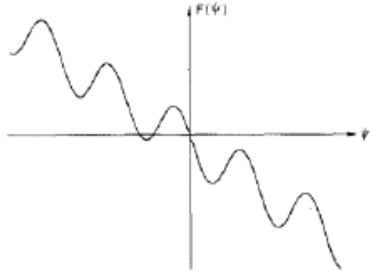

Fig. 1. The poderomotive potential $F(\psi)$. The case shown is for positive ψ_r corresponding to the case in which energy is extracted from the electrons.

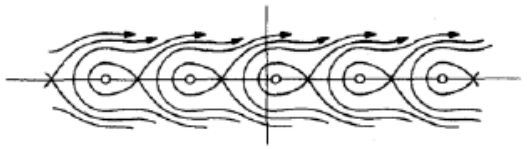

Fig. 2. Trajectories in the $\psi, \delta\gamma$ phase plane for $\psi_r > 0$.

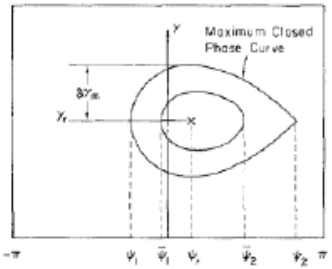

Fig. 3. Stable phase plane trajectories.

change in parameters is small. For small oscillations about ψ_r, one can expand $F(\psi)$ about ψ_r. The motion for these orbits is harmonic with period of oscillation

$$Z = \frac{\pi\mu}{(k_w + \delta k_s)\sqrt{a_s a_w \cos\psi_r}} \approx \frac{\mu\lambda_w}{2\sqrt{a_s a_w \cos\psi_r}}$$

$(\lambda_w \equiv 2\pi/k_w).$ (2.50)

Undulator tapering in the presence of diffraction effects

Nuclear Instruments and Methods in Physics Research A 375 (1996) 550–562

ELSEVIER

NUCLEAR INSTRUMENTS & METHODS IN PHYSICS RESEARCH Section A

''Optical guiding'' limits on extraction efficiencies of single-pass, tapered wiggler amplifiers☆

W.M. Fawley*

Lawrence Berkeley National Laboratory, University of California, 1 Cyclotron Rd., Berkeley, CA 94720, USA

Abstract

Single-pass, tapered wiggler amplifiers have an attactive feature of being able, in theory at least, of extracting a large portion of the electron beam energy into light. In circumstances where an optical FEL wiggler length is significantly longer than the Rayleigh length z_R corresponding to the electron beam radius, diffraction losses must be controlled via the phenomenon of optical guiding. Since the strength of the guiding depends upon the effective refractive index n exceeding one, and since $(n-1)$ is inversely proportional to the optical electric field, there is a natural limiting mechanism to the on-axis field strength and thus the rate at which energy may be extracted from the electron beam. In particular, the extraction efficiency for a prebunched beam asymptotically grows linearly with z rather than quadratically. We present analytical and numerical simulation results concerning this behavior and discuss its applicability to various FEL designs including oscillator/amplifier-radiator configurations.

$S_{\rm rad} \simeq r_{\rm b}^2 \qquad \text{for} \qquad r_{\rm dif}^2 \ll r_{\rm b}^2 .$

Assuming that a significant fraction of the particles is trapped in the regime of coherent deceleration, we can estimate the power loss by the electron beam in the tapered section as:

$$W \simeq I_0 |\tilde{E}| \theta_{\rm s} z_{\rm tap} .$$

In the latter expression we used the following estimation for the radiation field:

$$\int_0^{z_{\rm tap}} \tilde{E}(z) {\rm d}z \simeq \tilde{E}(z_{\rm tap}) z_{\rm tap} .$$

Thus, we have the following power balance:

1. Thin electron beam ($r_{\rm b}^2 \ll c z_{\rm tap}/\omega$):

$$S_{\rm rad} \sim c z_{\rm tap}/\omega ,$$

$$W \simeq I_0 |\tilde{E}| \theta_{\rm s} z_{\rm tap} \simeq |\tilde{E}|^2 c^2 z_{\rm tap}/\omega \quad \rightarrow$$

$$W \simeq I_0^2 \theta_{\rm s}^2 z_{\rm tap} \omega / c^2 , \quad |\tilde{E}| \simeq I_0 \theta_{\rm s} \omega / c^2 .$$

2. Wide electron beam ($r_{\rm b}^2 \gg c z_{\rm tap}/\omega$):

$$S_{\rm rad} \simeq r_{\rm b}^2 ,$$

$$W \simeq I_0 |\tilde{E}| \theta_{\rm s} z_{\rm tap} \simeq |\tilde{E}|^2 r_{\rm b}^2 \quad \rightarrow$$

$$W \simeq I_0^2 \theta_{\rm s}^2 z_{\rm tap}^2 / (c r_{\rm b}^2) , \quad |\tilde{E}| \simeq I_0 \theta_{\rm s} z_{\rm tap} / (c r_{\rm b}^2) .$$

Our estimates show that in the case of a thin electron beam, the radiation field, acting on the electrons, is almost constant along the undulator axis. The radiation power grows linearly with the length of the tapered section, $z_{\rm tap}$. Thus, we can conclude that the regime of coherent deceleration of the particles should take place only for a linear law of undulator tapering, i.e. the detuning $C(z)$ should change linearly with the z coordinate.

Let us consider the case of a large value of the diffraction parameter,

$$B = \Gamma \omega r_{\rm b}^2 / c \gg 1 .$$

At the beginning of the tapering section, when $\Gamma z_{\rm tap} \lesssim B$, we deal with the case of a wide electron beam and most of the radiation overlaps with the electron beam. When the length of the tapered section increases, the radiation expands out of the electron beam. When $\Gamma z_{\rm tap} \gg B$ we always fall in the region when diffraction effects are important, i.e. the electron beam becomes thin with respect to the radiation beam. Thus, we come to the conclusion that the asymptotically stable regime of coherent deceleration should occur only for a linear law of undulator tapering.

It is well known from early studies that:

- Radiation power grows linearly with the undulator length for the asymptote of thin electron beam (i.e., long undulator)
- Radiation power grows quadratically with the undulator length for the asymptote of wide electron beam (i.e., short undulator / initial stage of tapered regime).

E. Saldin, E. Schneidmiller, M. Yurkov, "The Physics of Free Electron Lasers", 2000 /

Undulator tapering in the presence of diffraction effects

The key element for understanding the physics of the undulator tapering are the properties of the radiation from modulated electron beam.

Indeed, in the case of tapered FEL the beam bunching is frosen (particles are trapped in the regime of coherent deceleration).

Thus, we deal with the electron beam modulated at the resonance wavelength.

If we know the radiation power of the modulated electron beam as function of the undulator length, we know the law of the undulator tapering.

The problem of the radiation of modulated electron beam has been solved ten years ago (Nucl. Instrum. and Methods A 539, 499 (2005)), and recently connected with the problem of the undulator tapering (Phys. Rev. ST AB 18 (2015) 030705)).

Radiation of modulated electron beam

- Radiation power of modulated electron beam:

$$W = \frac{2\pi^2 I_0^2 a_{\rm in}^2 \sigma^2}{c\lambda\lambda_{\rm u}} \frac{K^2 A_{\rm JJ}^2}{1+K^2} f(\tilde{z})\tilde{z}\,, \qquad f(\tilde{z}) = \arctan(\tilde{z}/2) + \tilde{z}^{-1}\ln\left(\frac{4}{\tilde{z}^2+4}\right)$$

- Thin and wide beam asymptote:

$$f(\tilde{z}) \to \pi/2 \qquad \text{for} \qquad \tilde{z} \gg 1 \qquad (N \ll 1)\,,$$
$$f(\tilde{z}) = \tilde{z}/4 \qquad \text{for} \qquad \tilde{z} \ll 1 \qquad (N \gg 1)\,.$$

The Fresnel number: $N = 2\pi\sigma^2/(\lambda z)$.

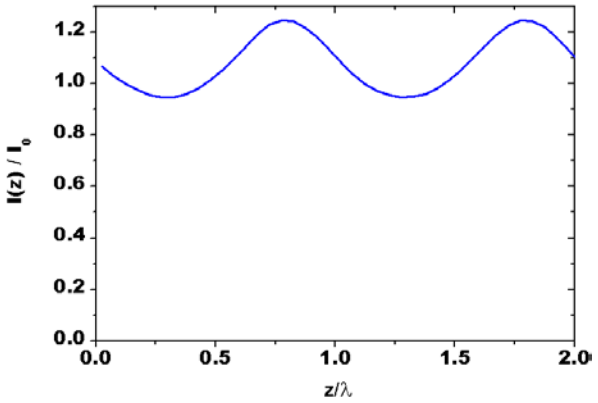

- Both asymptotes (of wide and thin electron beam) discussed in earlier papers are well described by this expression.
- Asymptote of a wide electron beam corresponds to large values of Fresnel number N, and the radiation power scales quadratically with the undulator length, $W \propto z^2$.
- Asymptote of a thin electron beam corresponds to small values of the Fresnel Number N, and the radiation power grows linearly with the undulator length, $W \propto z$.
- Undulator tapering should adjust detuning according to the energy loss by electrons, and we find that the tapering law should be quadratic for the case of wide electron beam, $C \propto W \propto z^2$, and linear for the case of thin electron beam, $C \propto W \propto z$.

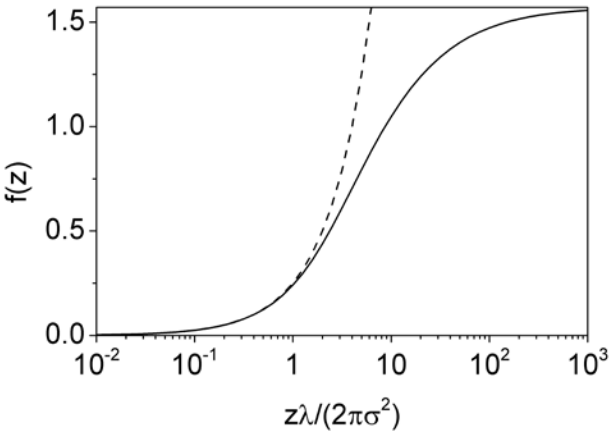

Radiation of modulated electron beam

- Radiation power of modulated electron beam:

$$W = \frac{2\pi^2 I_0^2 a_{\rm in}^2 \sigma^2}{c\lambda\lambda_{\rm u}} \frac{K^2 A_{\rm JJ}^2}{1+K^2} f(\tilde{z})\tilde{z}\,, \qquad f(\tilde{z}) = \arctan(\tilde{z}/2) + \tilde{z}^{-1}\ln\left(\frac{4}{\tilde{z}^2+4}\right).$$

Thin and wide beam asymptote:

$$f(\tilde{z}) \to \pi/2 \quad \text{for} \quad \tilde{z} \gg 1 \quad (N \ll 1)\,,$$
$$f(\tilde{z}) = \tilde{z}/4 \quad \text{for} \quad \tilde{z} \ll 1 \quad (N \gg 1)\,.$$

The Fresnel number: $N = 2\pi\sigma^2/(\lambda z)$.

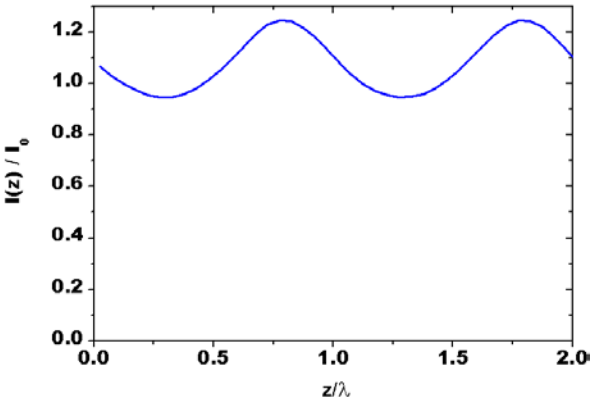

- Asymptote of the wide electron beam works reasonably well for the values of the Fresnel number $N \gtrsim 1$. Asymptote of the thin electron beam converges pretty slowly, and reasonable accuracy is achieved for very small $N \lesssim 0.01$.
- Example for LCLS operating at the radiation wavelength of 0.15 nm and 1.5 nm. Transverse size of the electron beam is about 25 μm in both cases.
- The wide beam asymptote is applicable up to $z \simeq z_{\rm wb} \simeq 26$ m for wavelength 0.15 nm, and $z \simeq z_{\rm wb} \simeq 2.6$ m for operation at 1.5 nm wavelength. Here we see general feature illustrating shortening with the radiation wavelength of the applicability region of the wide beam asymptote.
- The thin beam asymptote becomes to be applicable at LCLS for $z \gtrsim 2500$ m (for wavelength 0.15 nm) and 260 m (for wavelength 1.5 nm). Note, that for both practical examples the limit of thin electron beam is achieved only for very long undulator, and exact formula should be used for calculation of the radiation power for undulator length $z \gtrsim z_{\rm wb}$.

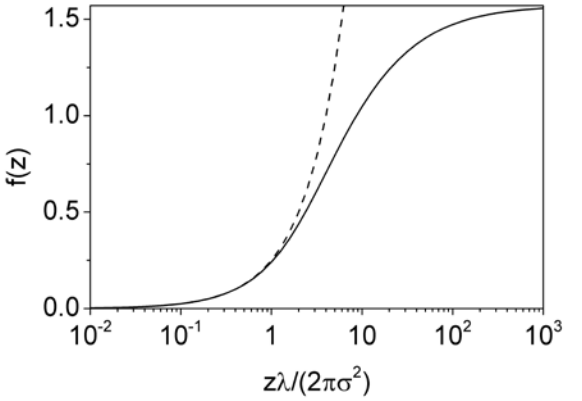

Application of similarity techniques

- In the framework of the three-dimensional theory the operation of the FEL amplifier is described by the diffraction parameter B, the energy spread parameter $\hat{\Lambda}_{\rm T}^2$, the betatron motion parameter $\hat{k}_\beta$ and detuning parameter $\hat{C}$:

$$B = 2\Gamma\sigma^2\omega/c\ , \qquad \hat{C} = C/\Gamma\ , \qquad \hat{k}_\beta = 1/(\beta\Gamma)\ , \qquad \hat{\Lambda}_{\rm T}^2 = (\sigma_{\rm E}/\mathcal{E})^2/\rho^2\ ,$$

with the gain parameter $\Gamma = 4\pi\rho/\lambda_w$. For the case of "cold" electron beam, $\hat{\Lambda}_{\rm T}^2 \to 0$, $\hat{k}_\beta \to 0$, the operation of the FEL amplifier is described by the diffraction parameter B and the detuning parameter $\hat{C}$.

- FEL equations:

$$\frac{d\Psi}{d\hat{z}} = \hat{C} + \hat{P}, \qquad \frac{d\hat{P}}{d\hat{z}} = U\cos(\phi_U + \Psi)\ ,$$

where $\hat{P} = (E - E_0)/(\rho E_0)$, $\hat{z} = \Gamma z$, and U and ϕ_U are the amplitude and the phase of the effective potential.

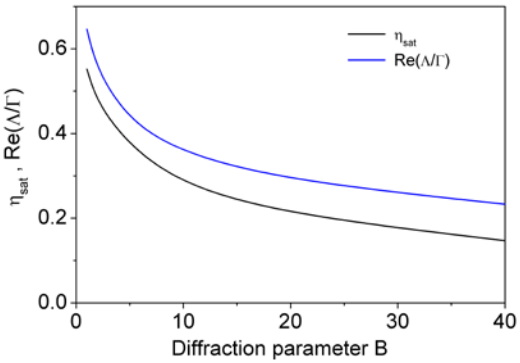

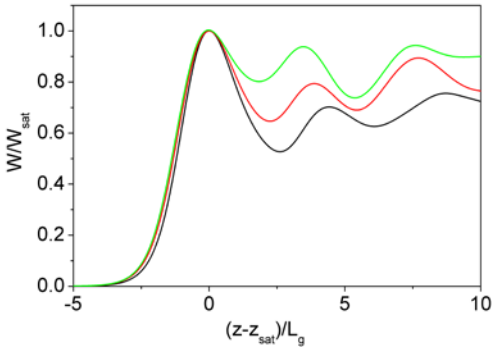

- We normalize the radiation power to the saturation power, and undulator length to the field gain length. Then we find that the radiation power before saturation exhibits similar behavior for all values of the diffraction parameter $B > 1$.

- In view of: i) universal scaling of the FEL characteristics on the diffraction parameter B; ii) The Fresnel number and the diffraction parameter has the same physical meaning, we find that optimum undulator tapering should be:

$$\hat{C} = \alpha_{tap}(\hat{z} - \hat{z}_0)\left[\arctan\left(\frac{1}{2N}\right) + N\ln\left(\frac{4N^2}{4N^2+1}\right)\right]\ , \qquad N = \frac{\beta_{tap}}{\hat{z} - \hat{z}_0}\ .$$

Global numerical optimization versus the universal law of the undulator tapering

- First, we perform straightforward global optimization with three-dimensional, time-dependent FEL simulation code FAST.
- Target of the optimization is maximum of the output power at 15 gain lengths after saturation. We divide undulator into many pieces and change detuning of all pieces independently. Number of sections is controlled to provide the result independent on the number of sections.
- We choose the tapering law $C(B, z)$ corresponding to the maximum power at the exit of the whole undulator.
- Then we fit parameters of the universal tapering law:

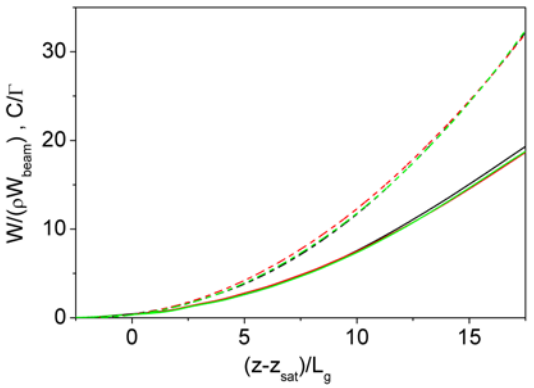

$$\hat{C} = \alpha_{tap}(\hat{z} - \hat{z}_0)\left[\arctan\left(\frac{1}{2N}\right) + N\ln\left(\frac{4N^2}{4N^2+1}\right)\right], \qquad N = \frac{\beta_{tap}}{(\hat{z} - \hat{z}_0)}$$

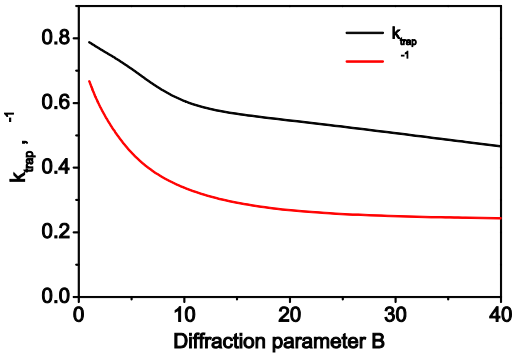

- Start of the undulator tapering z_0 is fixed by the global optimization procedure, $z_0 = z_{sat} - 2L_g$.
- Another parameter of the problem, β_{tap}, is rather well approximated with the linear dependency on the diffraction parameter, $\beta_{tap} = 8.5 \times B$.
- Remaining parameter, α_{tap}, is plotted in Figure. It is a slow varying function of the diffraction parameter B, and scales approximately to $B^{1/3}$ as all other important FEL parameters including capture efficiency.
- Thus, application of similarity techniques gives us an elegant way for the general parametrical fit.

Global numerical optimization versus the universal law of the undulator tapering and the rational fit

- Universal tapering law:

$$\hat{C} = \alpha_{tap}(\hat{z} - \hat{z}_0)\left[\arctan\left(\frac{1}{2N}\right) + N\ln\left(\frac{4N^2}{4N^2+1}\right)\right] ,$$

with Fresnel number N fitted by $N = \beta_{tap}/(\hat{z} - \hat{z}_0)$. Start of the undulator tapering is $z_0 = z_{sat} - 2L_g$. Parameter β_{tap}, is $\beta_{tap} = 8.5 \times B$.

- Expression for the universal tapering law has quadratic dependence in z for small values of z (limit of the wide electron beam), and linear dependence in z for large values of z (limit of the thin electron beam). It is natural to try a fit with a rational function which satisfies both asymptotes. The simplest rational fit is:

$$\hat{C} = \frac{a(\hat{z} - \hat{z}_0)^2}{1 + b(\hat{z} - \hat{z}_0)} .$$

- The coefficients a and b are the functions of the diffraction parameter B, and are plotted in the Figure. Start of the undulator tapering is set to the value $z_0 = z_{sat} - 2L_g$ suggested by the global optimization procedure.

- Lower Figure: evolution along the undulator of the reduced radiation power $\hat{\eta} = W/(\rho W_{\rm beam})$ (solid curves) and of the detuning parameter $\hat{C} = C/\Gamma$ (dashed curves). Color codes: black - FEL with global optimization of undulator tapering, red - fit with the universal tapering law, green - fit with the rational function. The value of the diffraction parameter is $B = 10$.

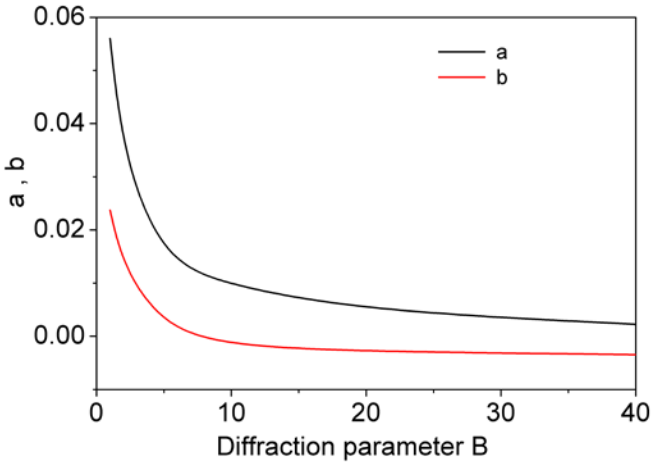

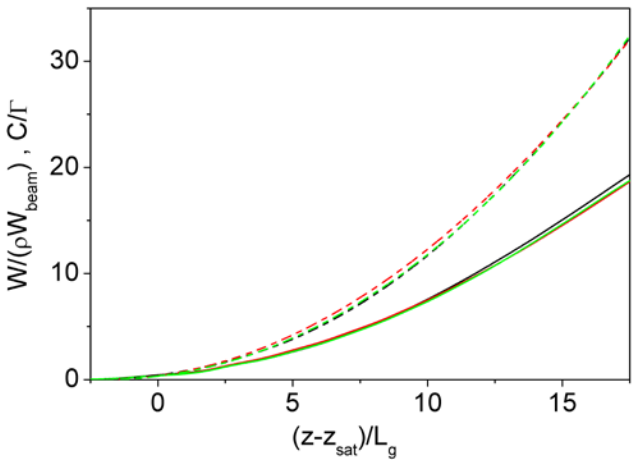

Trapping process for optimum tapering: how it works

Top: tapered

Bottom: untapered

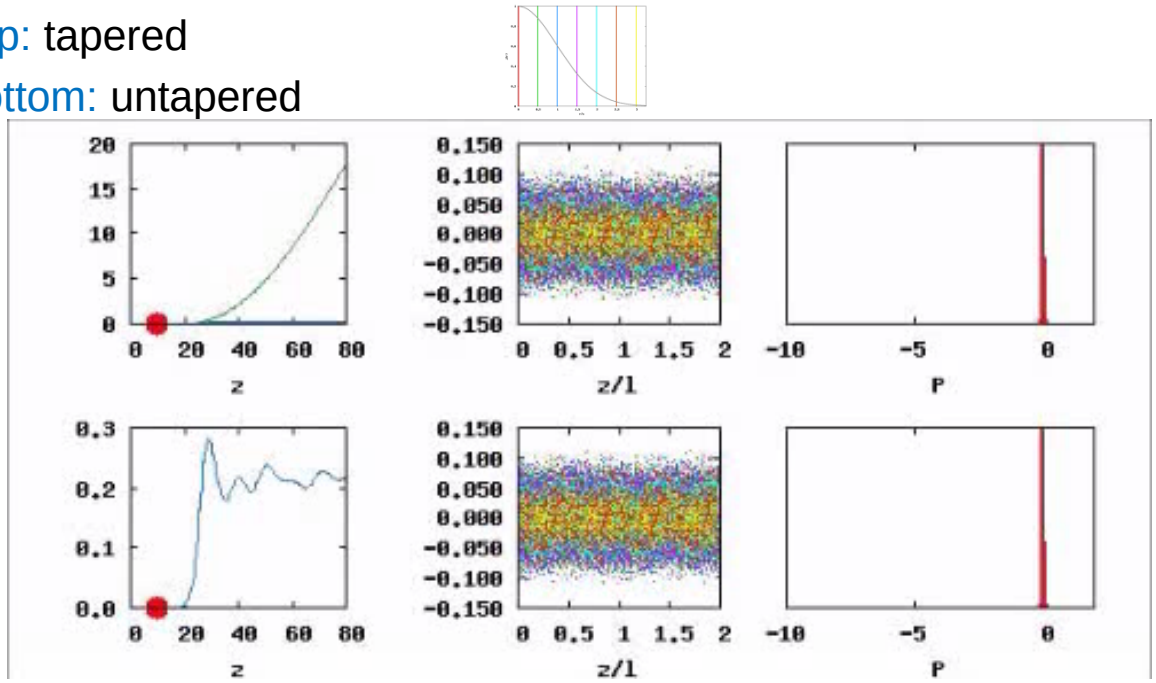

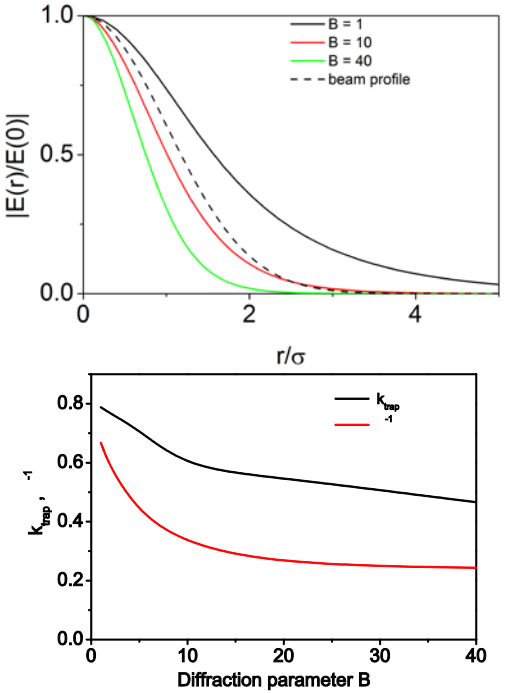

- The particles in the core of the beam (red, green, blue color) are trapped most effectively. Nearly all particles located at the edge of the electron beam (braun, yellow color) leave the stability region very soon. The trapping process lasts for a several field gain lengths when the trapped particles become to be isolated in the trapped energy band for which the undulator tapering is optimized further. Non-trapped particles continue to populate low energy tail of the energy distribution.

- Experimental observation at LCLS: energy distribution of non-trapped particles is not uniform, but represent a kind of energy bands. Our simulations give a hint on the origin of energy bands which are formed by non-trapped particles. This is the consequence of nonlinear dynamics of electrons leaving the region of stability. Note that a similar effect can be seen in the early one-dimensional studies.

Trapping process

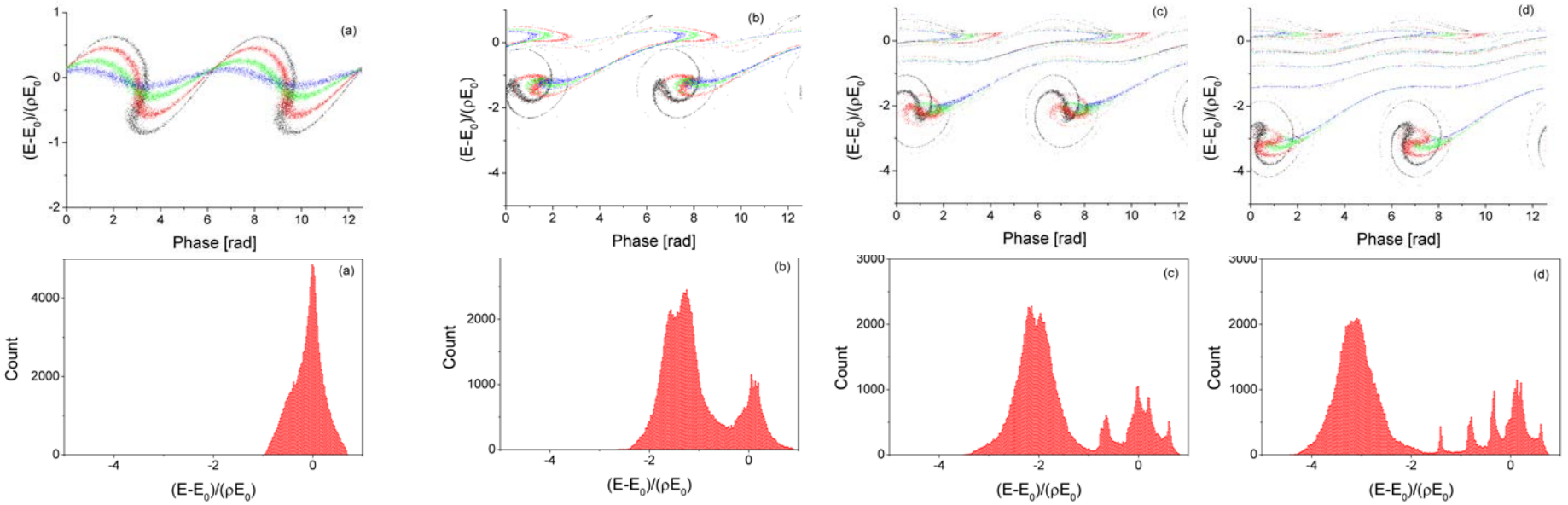

- The trapping efficiency falls down with the value of the diffraction parameter B. This is natural consequence of the diffraction effects. Variation of the FEL radiation mode (and the amplitude of ponderomotive well) across the electron beam is more pronouncing for larger values of the diffraction parameter B.

- The particles in the core of the beam (black points) are trapped most effectively. Nearly all particles located at the edge of the electron beam (blue points) leave the stability region very soon. The trapping process lasts for a several field gain lengths when the trapped particles become to be isolated in the trapped energy band for which the undulator tapering is optimized further. Non-trapped particles continue to populate low energy tail of the energy distribution.

- Experimental observation at LCLS: energy distribution of non-trapped particles is not uniform, but represent a kind of energy bands. Our simulations give a hint on the origin of energy bands which are formed by non-trapped particles. This is the consequence of nonlinear dynamics of electrons leaving the region of stability. Note that a similar effect can be seen in the early one-dimensional studies.

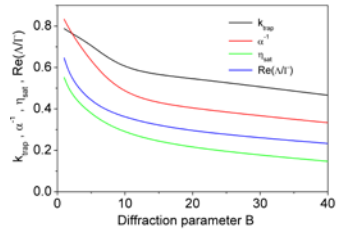

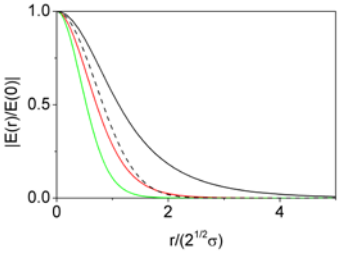

Energy bands in early 1D simulations

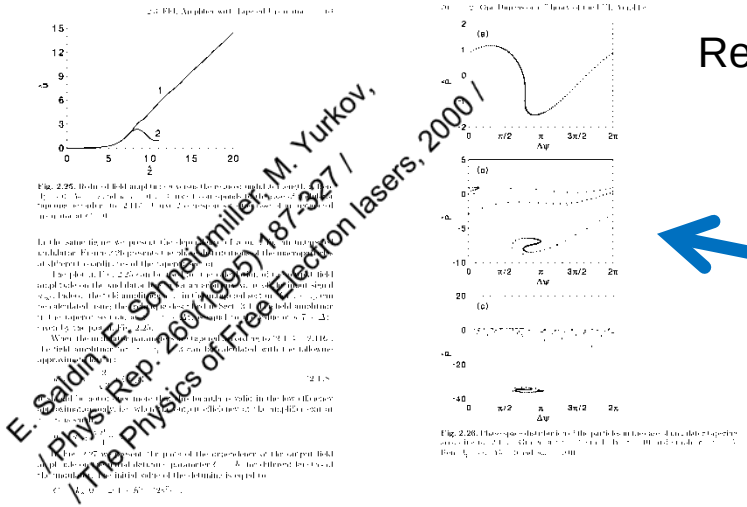

Revisited: the same code (FAST), just more macroparticles

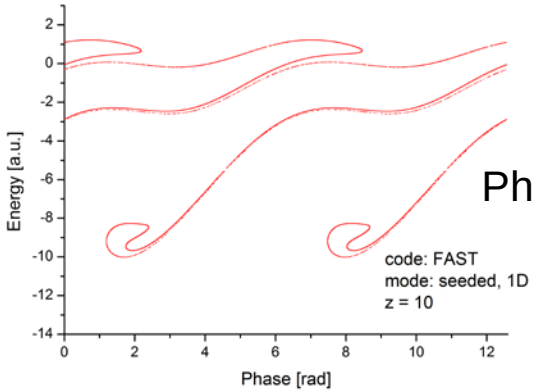

Phase space

Tutorial example from a book (1D FEL theory)

Energy spectrum

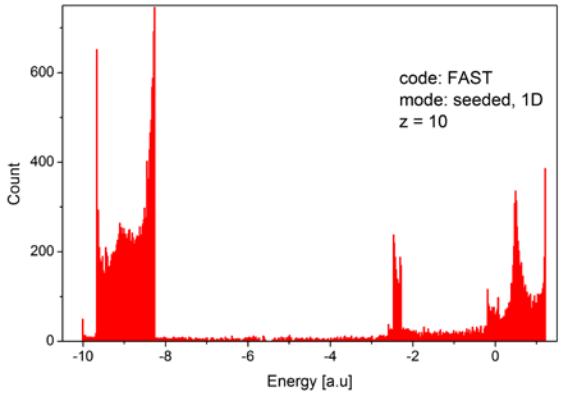

SASE FEL: Optimum tapering

- Radiation of SASE FEL consists of wavepackets (spikes). In the exponential regime of amplifications wavepackets interact strongly with the electron beam, and their group velocity $\mathrm{d}\,\omega/\mathrm{d}\,k$ visibly differs from the velocity of light, and the slippage of the radiation with respect to the electron beam is by several times less than kinematic slippage. I.e., wavepackets are closely connected with the modulations of the electron beam current.

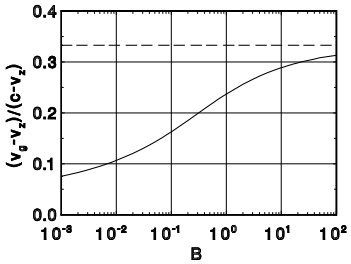

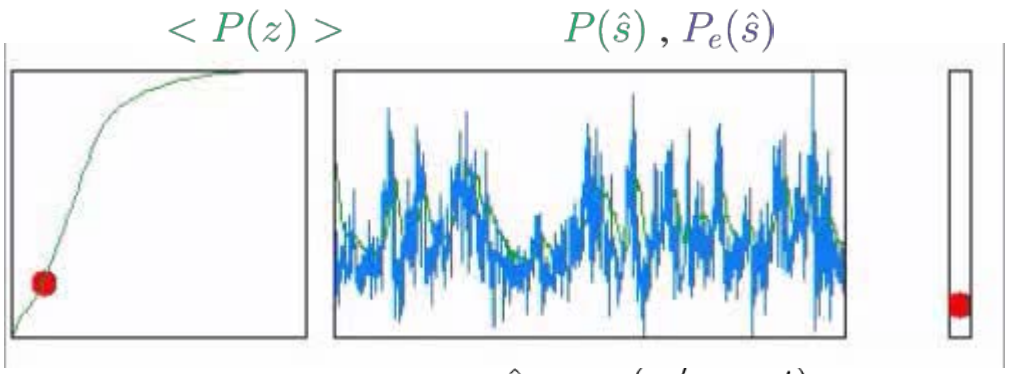

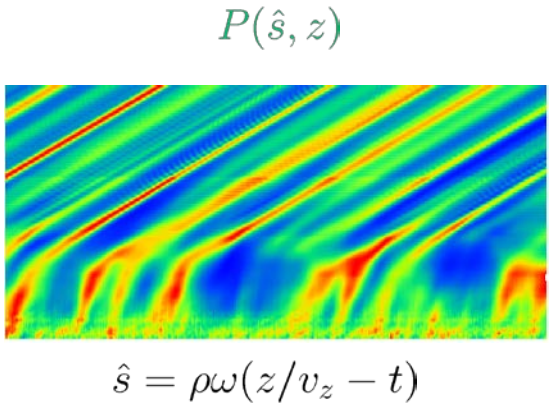

- When the amplification process enters nonlinear (tapering) stage, the group velocity of the wavepackets approaches to the velocity of light, and the relative slippage approaches to the kinematic one. When a wavepacket advances such that it reaches the next area of the beam disturbed by another wavepacket, we can easily predict that the trapping process will be destroyed, since the phases of the beam bunching and of the electromagnetic wave are uncorrelated in this case.

- Typical scale for the destruction of the tapering regime is coherence length, and the only physical mechanism we can use is to decrease the group velocity of wavepackets. This happens optimally when we trap maximum of the particles in the regime of coherent deceleration, and force these particles to interact as strong as possible with the electron beam. Thus, the strategy is exactly the same as we used for optimization of seeded FEL.

- Conditions of the optimum tapering for SASE are similar to those of the seeded case. Start of the tapering is by two field gain lengths before the saturation. Parameter β_{tap} is the same, $8.5 \times B$. The only difference is the reduction of the parameter α_{tap} by 20% which is natural if one remember statistical nature of the wavepackets.

SASE FEL, optimum tapering: how it works

- Left: slice radiation power and energy loss; phase space
- Right: bunching, average power, particle energy spectrum

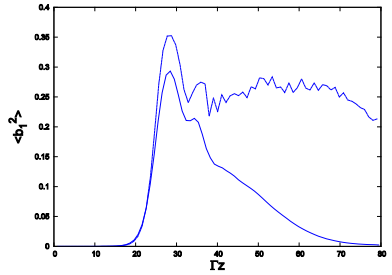

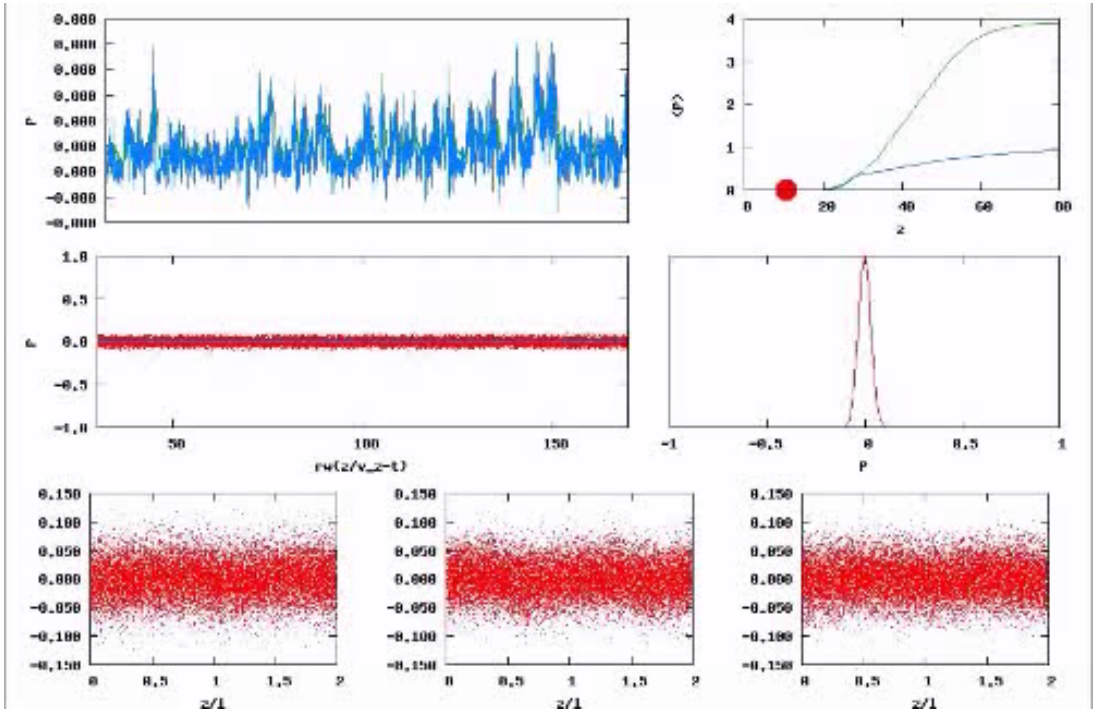

Bunching

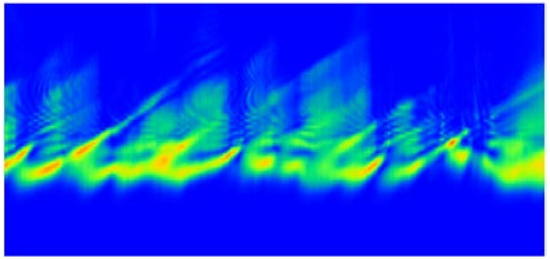

Radiation power

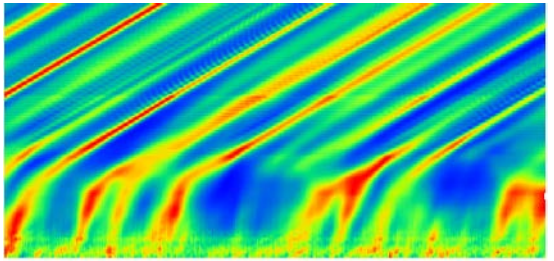

Energy loss

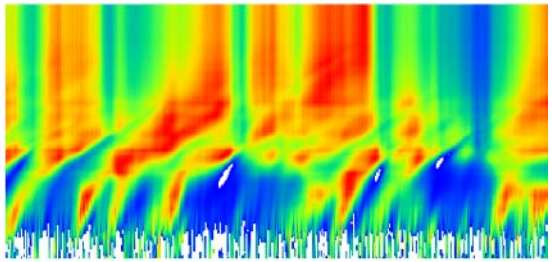

z

z

$$\hat{C} = \alpha_{tap}(\hat{z} - \hat{z}_0)\left[\arctan\left(\frac{1}{2N}\right) + N\ln\left(\frac{4N^2}{4N^2+1}\right)\right], \qquad N = \frac{\beta_{tap}}{(\hat{z}-\hat{z}_0)}$$

$$\hat{s} = \rho\omega(z/v_z - t)$$

Properties of the radiation: Optimum tapered versus untapered case

- Practical example: European XFEL, SASE3, radiation wavelength 1.6 nm.
- General feature of tapered regime is that both, spatial and temporal coherence degrade in the nonlinear regime, but a bit slowly than for untapered case.
- Peak brilliance grows due to the growth of the radiation power, and reaches maximum value in the middle of tapered section. Benefit in the peak brilliance is about factor of 3 with respect to untapered case.

Power and brilliance

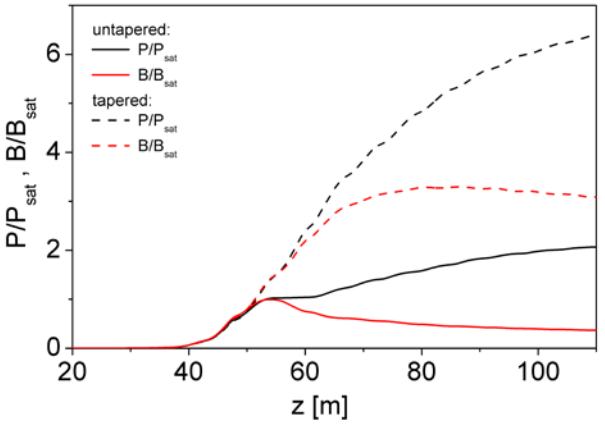

Degree of transverse coherence

Coherence time

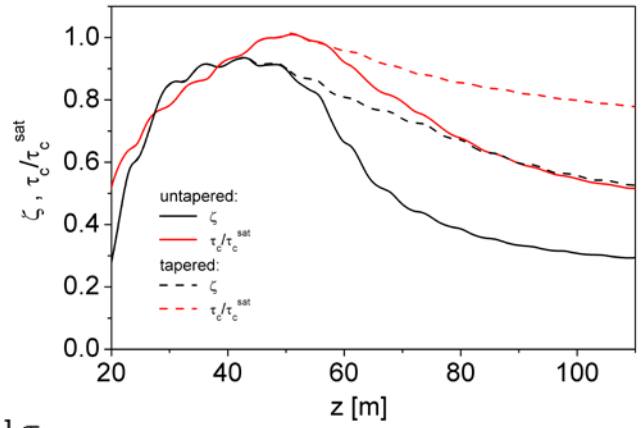

- Spatial corellations and degree of transverse coherence:

$$\gamma_1(\vec{r}_\perp, \vec{r}\prime_\perp, z, t) = \frac{\langle \tilde{E}(\vec{r}_\perp, z, t)\tilde{E}^*(\vec{r}\prime_\perp, z, t)\rangle}{\left[\langle|\tilde{E}(\vec{r}_\perp, z, t)|^2\rangle\langle|\tilde{E}(\vec{r}\prime_\perp, z, t)|^2\rangle\right]^{1/2}} ,$$

$$\zeta = \frac{\int |\gamma_1(\vec{r}_\perp, \vec{r}\prime_\perp)|^2 I(\vec{r}_\perp) I(\vec{r}\prime_\perp)\, \mathrm{d}\vec{r}_\perp\, \mathrm{d}\vec{r}\prime_\perp}{\left[\int I(\vec{r}_\perp)\, \mathrm{d}\vec{r}_\perp\right]^2} ,$$

- Temporal corellations and coherence time:

$$g_1(\vec{r}, t - t') = \frac{\langle \tilde{E}(\vec{r}, t)\tilde{E}^*(\vec{r}, t')\rangle}{\left[\langle|\,\tilde{E}(\vec{r}, t)\,|^2\rangle\langle|\,\tilde{E}(\vec{r}, t')\,|^2\rangle\right]^{1/2}} , \qquad \tau_c = \int_{-\infty}^{\infty} |g_1(\tau)|^2\, \mathrm{d}\tau .$$

FLASH2: Undulator tapering for efficiency increase

Use of statistical measurements for tuning optimum undulator tapering:

- Optimum conditions of the undulator tapering assume the starting point to be by two field gain lengths before the saturation point (corresponding to the maximum brilliance of the SASE FEL radiation).
- Saturation point on the gain curve is defined by the condition for fluctuations to fall down by a factor of 3 with respect to their maximum value in the end of exponential regime.
- Then quadratic law of tapering is applied (optimal for moderate increase of the extraction efficiency at the initial stage of tapering).

Experimental results from FLASH 2, January-May 2016

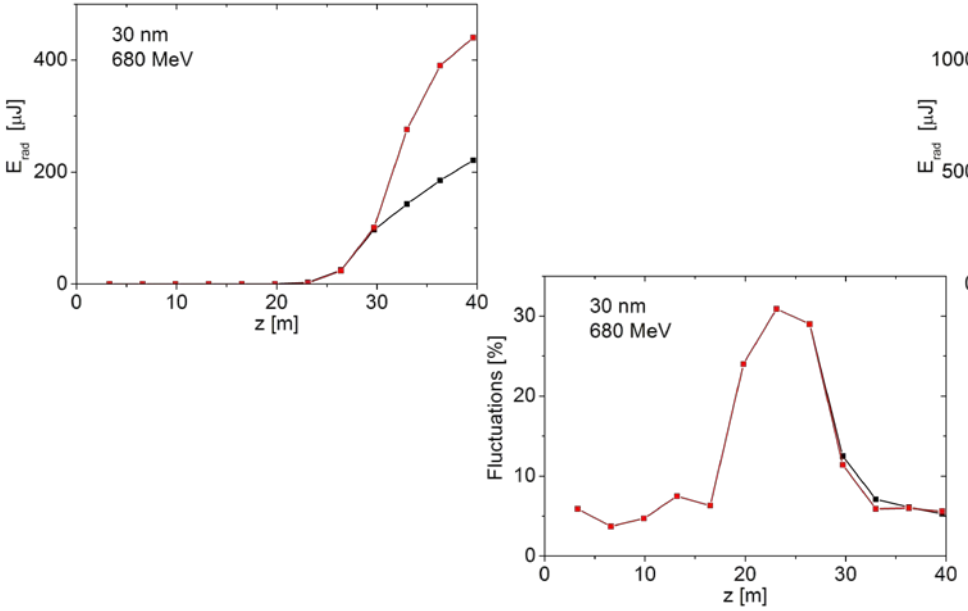

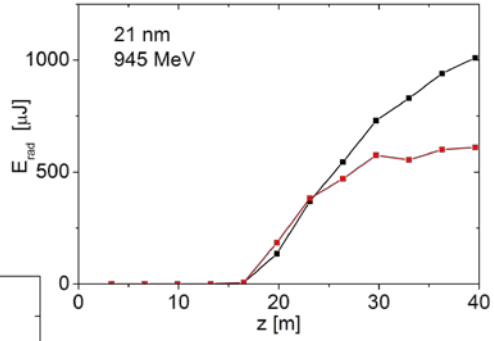

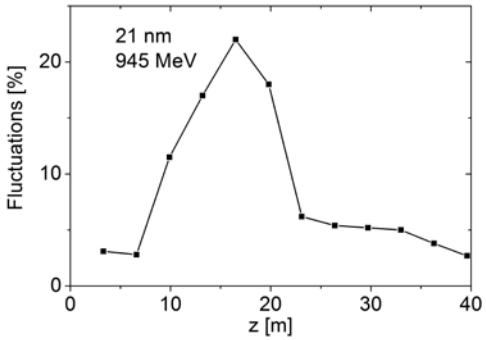

Undulator tapering in presence of diffraction effects: Conclusion

- The general law for optimum undulator tapering in the presence of diffraction effects is simple analytical expression with two fitting coefficients
- Key elements are knowledge of the radiation properties of modulated electron beam and application of similarity techniques in the FEL theory.
- Investigation of the case of “cold” electron beam allows one to isolate diffraction effects in the most clear form, and the optimum tapering law is the function of the only diffraction parameter B.
- Extension of this approach with including energy spread and emittance effects is straightforward and will result just in corrections to the fitting coefficients without changing the general law as we demonstrated for the case of SASE FEL.

Summary

Undulator tapering is a powerful tool for control properties of the radiation and for extending experimental capabilities. It can be used for:

- Compensation of the beam energy loss due to spontaneous undulator radiation.
- Compensation of the energy chirp in the electron beam.
- Increase power of a high-gain FEL after saturation (post-saturation taper) and FEL oscillators.
- Suppression of the radiation from the main undulator for organization of effective operation of afterburners (e.g., circular polarization).
- Application in the scheme of attosecond SASE FEL.

Thank you very much for your attention!

Literature sources used or referenced in the talk

The talk is based on:

E.A. Schneidmiller, and M.V. Yurkov, Optimization of a high efficiency free electron laser amplifier, Phys. Rev. ST Accel. Beams 18 (2015) 030705.

E.A. Schneidmiller, and M.V. Yurkov, The universal method for optimization of undulator tapering in FEL amplifiers, Proc. SPIE Vol. 9512, 951219 (2015).

E.A. Schneidmiller, and M.V. Yurkov, Optimization of a high efficiency free electron laser amplifier, Proc. FEL2015, MOC02.

E.A. Schneidmiller, and M.V. Yurkov, Application of Statistical Methods for Measurements of the Coherence Properties of the Radiation from SASE FEL, Proc. IPAC2016, MOPOW013.

Undulator tapering for efficiency increase(FEL amplifier):

N.M. Kroll, P.L. Morton, and M.N. Rosenbluth, IEEE J. Quantum Electron. 17, 1436 (1981).

T.J. Orzechowski, B.R. Anderson, J.C. Clark, W.M. Fawley, A.C. Paul, D. Prosnitz, E.T. Scharlemann, S.M. Yarema, D.B. Hopkins, A.M. Sessler, and J.S. Wurtele, Phys. Rev. Lett. 57, 2172 (1986).

R.A. Jong, E.T. Scharlemann, W.M. Fawley Nucl. Instrum. Methods Phys. Res. A272, 99 (1988)

W.M. Fawley, Nucl. Instrum. Methods Phys. Res. A375, 550 (1996)

E.L. Saldin, E.A. Schneidmiller and M.V. Yurkov, Opt. Commun. 95, 141 (1993).

E.L. Saldin, E.A. Schneidmiller, M.V. Yurkov, "The Physics of Free Electron Lasers" (Springer-Verlag, Berlin, 1999).

Y. Jiao, J. Wu, Y. Cai, A. W. Chao, W. M. Fawley, J. Frisch, Z. Huang, H.-D. Nuhn, C. Pellegrini, and S. Reiche, Phys. Rev. ST Accel. Beams 15, 050704 (2012).

G. Geloni, V. Kocharyan, and E. Saldin, DESY Report 11-049, 2011.

I.V. Agapov, G. Geloni, G. Feng, V. Kocharyan, E. Saldin, S. Serkez, I. Zagorodnov, DESY Report 14-047; Proc. 2014 FEL Conference, Basel, Switzerland, 2014, MOP056.

Undulator tapering for efficiency increase (FEL oscillator, negative tapering):

E.L. Saldin, E.A. Schneidmiller, M.V. Yurkov, Opt. Commun. 103, 297 (1993)

E.L. Saldin, E.A. Schneidmiller, M.V. Yurkov, Nucl. Instrum. Methods Phys. Res. A 375, 336 (1996)

S. Benson, J. Gubeli, G.R. Neil, Nucl. Instrum. Methods Phys. Res. A 475, 276 (2001)

LCLS - experimental results on tapering:

Y. Ding, F.-J. Decker, V.A. Dolgashev, J. Frisch, Z. Huang, P. Krejcik, H. Loos, A. Lutman, A. Marinelli, T.J. Maxwell, D. Ratner, J. Turner, J. Wang, M.-H. Wang, J. Welch, and J. Wu, Preprint SLAC-PUB-16105, SLAC National Accelerator Laboratory, 2014.

Application of negative tapering (attosecond pulses, helical afterburner):

E.L. Saldin, E.A. Schneidmiller, M.V. Yurkov, Phys. Rev. ST Accel. Beams 9, 050702 (2006)).

E.A. Schneidmiller, M.V. Yurkov, Phys. Rev. ST Accel. Beams 16, 110702 (2013).

E.A. Schneidmiller and M.V. Yurkov, Reverse undulator tapering for polarization controls at XFELs, Proc. IPAC2016, MOPOW008.

A.A. Lutman et al, Polarization control in an X-ray free-electron laser, Nature Photonics, Published online 09 May 2016, 1038/nphoton.2016.79.

General topics of FEL physics:

E.L. Saldin, E.A. Schneidmiller and M.V. Yurkov, Physics Reports 260, 187 (1995).

E.L. Saldin, E.A. Schneidmiller, M.V. Yurkov, "The Physics of Free Electron Lasers" (Springer-Verlag, Berlin, 1999).

P. Schmueser, M. Dohlus, J. Rossbach, C. Behrens, Free-Electron Lasers in the Ultraviolet and X-Ray Regime (Springer-Verlag, Berlin, 2014).

Z. Huang and K.-J. Kim, Review of x-ray free electron laser theory, Phys. Rev. ST Accel. Beams 10(2007)034801.

Backup slides

Properties of the radiation: tapered versus untapered
SASE3: 1.6 nm @ 14 GeV

#						
Electron beam:						
#						
Energy of electrons	GeV	14.0				
Bunch charge	nC	.200E-01	.100	.250	.500	1.00
Peak current	kA	4.50	5.00	5.00	5.00	5.00
rms normalized emittance	mm-mrad	.320	.390	.600	.700	.970
rms energy spread	MeV	4.10	2.90	2.50	2.20	2.00
rms bunch length	micrometr	.360	1.92	4.98	9.17	23.0
Focusing beta function	m	15.0	15.0	15.0	15.0	15.0
rms size of electron beam	micrometr	13.2	14.6	18.1	19.6	23.0
Repetition rate	1/sec	.270E+05				
Electron beam power	kW	7.56	37.8	94.5	189.	378.
#						
Undulator:						
#						
Undulator period	cm	6.80				
Undulator peak field	T	1.30				
Undulator parameter K (rms)	#	5.86				
Undulator length	m	105.				
#						
Properties of the 1st harmonic in the saturation:						
#						
Radiation wavelength	nm	1.60				
Photon energy	keV	.775				
Pulse energy	mJ	.166	1.01	2.38	4.24	9.71
Peak power	W	99.0	113.	102.	99.0	90.5
Average power	W	4.49	27.4	64.3	115.	262.
FWHM spot size	mikrometr	41.6	44.8	53.4	56.8	64.8
FWHM angular divergence	microrad	16.6	16.0	14.2	13.5	12.3
Coherence time	fs	.824	.817	.909	.945	1.03
FWHM spectrum width, dw/w	%	.458	.462	.415	.399	.365
Degree of transverse coherence	#	.960	.960	.960	.960	.960
Radiation pulse duration	fs	1.68	8.96	23.2	42.8	107.
Number of longitudinal modes	#	2	11	26	45	104
Fluctuations of the pulse energy	%	23.6	10.1	6.54	4.97	3.27
Degeneracy parameter	#	.630E+12	.715E+12	.720E+12	.723E+12	.723E+12
Number oh photons per pulse	#	.134E+13	.817E+13	.192E+14	.341E+14	.782E+14
Average flux of photons	ph/sec	.361E+17	.220E+18	.517E+18	.922E+18	.211E+19
Peak brilliance	#	.261E+33	.296E+33	.298E+33	.299E+33	.299E+33
Average brilliance	#	.118E+23	.716E+23	.187E+24	.346E+24	.867E+24
Saturation length	m	38.5	38.2	42.7	44.4	48.6
Power gain length	m	1.75	1.73	1.91	1.99	2.17
SASE induced energy loss	MeV	22.0	22.6	20.5	19.8	18.1
SASE induced energy spread	MeV	56.2	57.8	52.3	50.5	46.2
#						

E. Schneidmiller, M. Yurkov, DESY 11-152

Properties of the radiation: tapered versus untapered
SASE3: 1.6 nm @ 14 GeV

1st harmonic

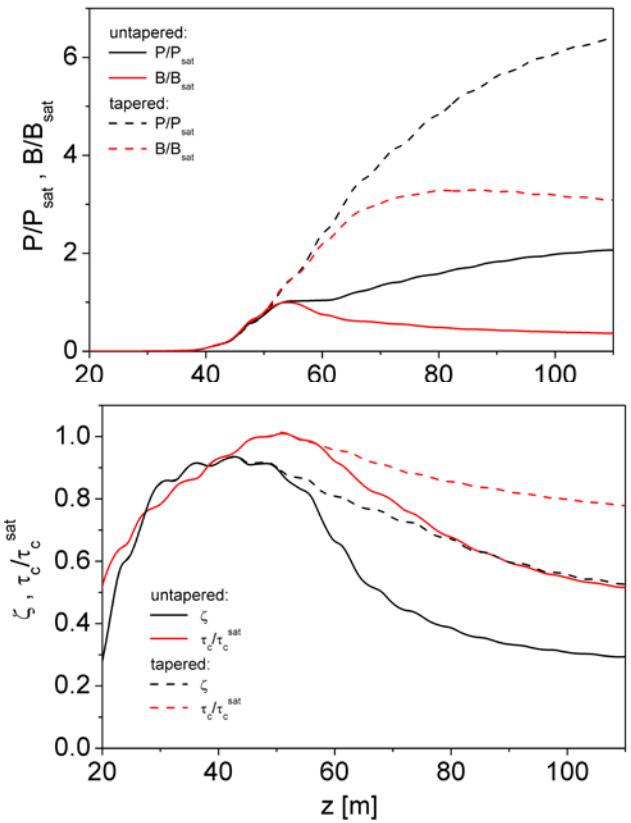

3rd harmonic

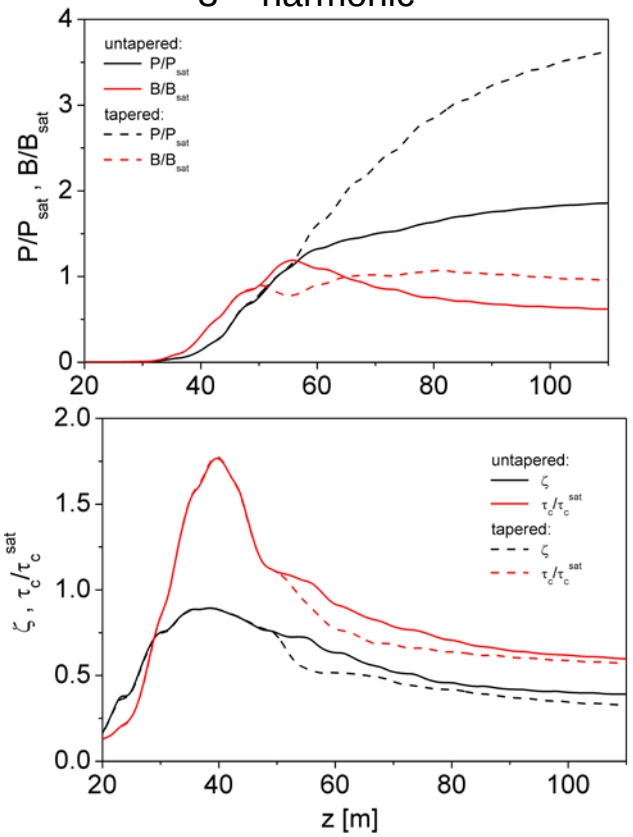

- Power, brilliance, coherence time, degree of transverse coherence.
- 1st harmonic. Parameters of the radiation at the saturation point are: the radiation power is 108 GW, the coherence time is 1.2 fs, the degree of transverse coherence is 0.86, and the brilliance of the radiation is equal to 3.8×10^{22} photons/sec/mm^2/rad^2/0.1% bandwidth.
- 3rd harmonic. Parameters of the radiation at the saturation point are: the radiation power is 6.6 GW, the coherence time is 0.5 fs, the degree of transverse coherence is 0.72.

Properties of the radiation: tapered versus untapered
SASE3: 1.6 nm @ 14 GeV

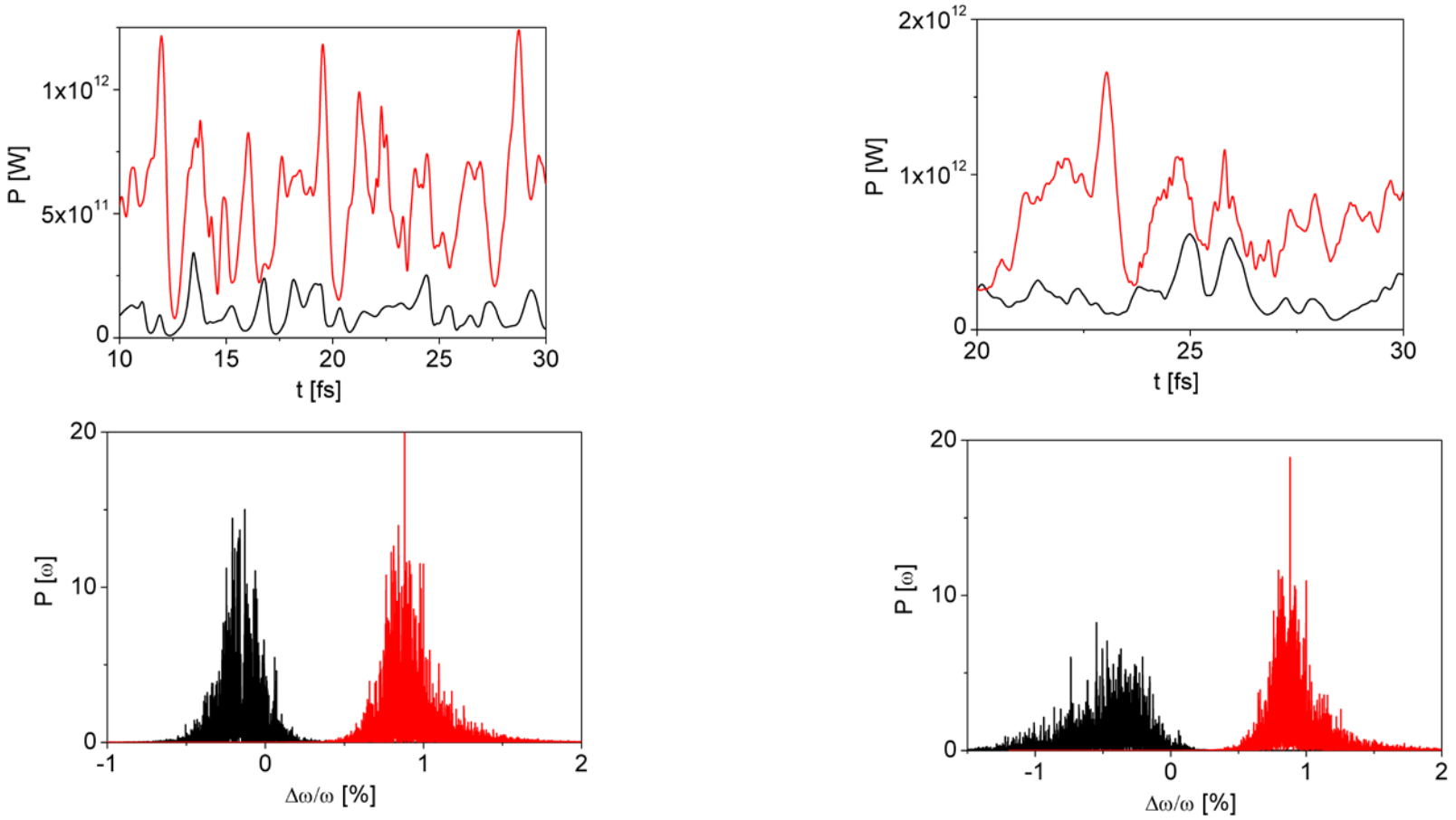

- Qualitative comparison of the temporal and spectral structure of the radiation for saturation points (left) and at the end of the undulator (right).

Properties of the radiation: tapered versus untapered
SASE3: 1.6 nm @ 14 GeV

Summary of the radiation properties:

- Application of the undulator tapering has evident benefit for SASE3 FEL operating in the wavelength range around 1.6 nm. It is about factor of 6 in the pulse radiation energy with respect to the saturation regime, and factor of 3 with respect to the radiation power at a full length.
- General feature of tapered regime is that both, spatial and temporal coherence degrade in the nonlinear regime, but more slowly than for untapered case.
- Peak brilliance is reached in the middle of tapered section, and exceeds by a factor of 3 the value of the peak brilliance in the saturation regime.

  The degree of transverse coherence at the saturation for untapered case is 0.86. The degree of transverse coherence for the maximum brilliance of the tapered case is 0.66.
- Coherence time falls by 15%.
- At the exit of the undulator the degree of transverse coherence for the tapered case is 0.6, and coherence time falls by 20%.
- Radiation of the 3rd harmonic for both, untapered and tapered cases, exhibit nearly constant brilliance and nearly constant contribution to the total power.
- Coherence time of the 3rd harmonic for the tapered case approximately scales inversely proportional to harmonic number, as in untapered case.